Confocal And Multiphoton Imaging Of Intracellular Ca^{2+}

Godfrey Smith[1], Martyn Reynolds[2], Francis Burton[1], Ole Johan Kemi[1]

[1]Faculty of Biomedical and Life Sciences, University of Glasgow, United Kingdom
[2]Cairn Research Limited, Faversham, Kent, United Kingdom

This chapter is to considers the practical issues associated with making confocal Ca^{2+} measurements in isolated cells and tissues. In the initial part of this chapter, we will discuss the strengths and weaknesses of available imaging modalities. In the next section we consider the issues associated with measurement/imaging of intracellular Ca^{2+} both in terms of dye calibration and the errors associated with quantifying [Ca^{2+}]. Finally, there is a section considering the practical issues attempting to image intracellular Ca^{2+} and transmembrane voltage simultaneously in cells.

Why Study Ca^{2+} Signaling With Confocal And Multiphoton Microscopy

Ca^{2+} is a ubiquitous intracellular messenger that controls a large number of cellular processes, such as gene transcription, excitation, contraction, apoptosis, cellular respiration, and the activity levels of many cell signaling messenger cascades. Inside the cell, Ca^{2+} may under various conditions sequester into the sarco/endoplasmic reticulum, mitochondria, and the nucleus, or exist in the cytosol either in its free form or as bound to buffers. Typically, a large Ca^{2+} concentrations gradient is maintained across the plasma membrane of the cell. Because of different Ca^{2+} channels, pumps, and exchangers on the membranes of the cell or organelles, Ca^{2+} fluxes may be created at multiple locations in the cell. Therefore Ca^{2+} concentration and signal may be specific with respect to both location and time. Moreover, Ca^{2+} may concentrate in distinct cytoplasmic regions because of tight physical loci not enclosed by membranes, e.g. the dyadic area between the transverse tubule and the sarco/endoplasmic reticulum of muscle cells. Given the large number of Ca^{2+} channels feeding it with Ca^{2+} from both the extracellular space (transverse tubule) and the sarco/endoplasmic reticulum, such that the dyad may transiently have very different localized Ca^{2+} concentrations compared to the rest of the cytosol which may be only nanometres away. Thus, Ca^{2+} localization in the cytosol and organellar

compartments may last for a wide range of periods, from nanoseconds to minutes. The average Ca^{2+} concentration in any given cell usually ranges from 0.1-1 μM, but that the Ca^{2+} almost never exists uniformly throughout the cell, and local Ca^{2+} events may occur very rapidly, requiring Ca^{2+} imaging of live specimens with high spatial and temporal resolution. Thus, one would ideally want to distinguish Ca^{2+} in distinct areas that may be within a nanometre distance from each other, and to record localized Ca^{2+} events that may only last milliseconds. Current confocal and multiphoton microscopy systems offer a range of imaging capabilities that partially fulfil these criteria.

Confocal Microscopy

Optical sectioning by confocal microscopy adds several benefits to Ca^{2+} imaging, it allows the study of events within discrete sections of cell or tissue by blocking light originating outside the plane of focus. This is achieved by the addition of an confocal apertures in front of the illumination source and in the image plane directly in front of the signal detection system (see Figure 1), usually a photomultiplier tube (PMT) that rejects out-of-focus light originating from fluorescence outside the area of interest (the focal plane), and only allowing in-focus light through to the detector (Webb 1999) (Figure 1). This is in contrast to regular epifluorescence microscopy, in which the majority of the fluorescence from a specimen is out-of-focus light, this reduces the contrast of the in-focus light and dramatically compromises in-focus detail. This occurs since the emitted fluorescence cannot be discriminated along the Z-axis (Lichtman and Conchello 2005).

Figure 1.

The difference between regular epifluorescence and confocal microscopy light capture abilities can be illustrated by the following examples. Considering that the depth of focus of a high numerical aperture (NA >1.3) objective is restricted to ~0.3 μm, whereas a cell may be ~5-25 μm deep, it is clear that the depth of focus constitutes only ~1-5% of the full depth of the cell. Since epifluorescence microscopy captures light along the entire Z-axis, 95-99% of the cell volume will contribute with unwanted out-of-focus background signal -effectively noise (Lichtman and Conchello 2005), that cannot be distinguished from in-focus fluorescence. However in theory, setting the pinhole of the confocal aperture to 1 Airy unit to achieve true confocality will

provide an optical section. Here a minimum of out-of-focus light will reach the signal detector, without any other interference to the optical pathway or any digital processing of the signal at the time of recording secondarily to the scanning and building of the image itself, which would compromise the scanning speed.

Nevertheless, resolution in 3D is diffraction limited as determined by the point spread function (PSF) set by the optical performance of the microscope. With high NA objectives (>1.2), XYZ resolution is typically ~0.3 x 0.3 x 0.6 μm (Cox and Sheppard 2004). Thus, although Z-resolution is dramatically different between conventional epifluorescence and confocal microscopes, the 2-dimensional (2D) spatial resolution in the XY-field is not, though factors such as excitation wavelength, objectives and the optical pathway, and different media and surfaces will also affect this. However, several aspects of the confocal principle allow for improving also XY-resolution, as compared to widefield epifluorescence microscopy. First, spatial resolution may be improved by further reducing the pinhole diameter to less than the width of the central disk of the Airy unit pattern, though this also dramatically reduces light transmission. This works because the pinhole is aligned with the centre of the Airy unit pattern of the illuminating beam, which means that any emission originating from any fluorophores excited by the outer airy rings of the illuminating beam will be blocked by the confocal aperture. Thus the resultant fluorescence emission may be manipulated to originate from an area smaller than the airy unit, which cannot be achieved by conventional widefield epifluorescence microscopy. Moreover, because the PSF of the confocal microscope is narrower at normalized light intensities relative to that of the conventional widefield microscope, the XY spatial resolution will be ~1.4 x greater with a confocal microscope than a widefield microscope (Conchello and Lichtman 2005). Finally, some of the in-focus light will scatter on its way through the specimen, due to diffraction, reflection, and refraction by cell structures. This compromises fluorescence, but not confocality, as the pinhole also blocks scattered light from reaching the signal detector.

Combining confocal microscopy with total internal reflection fluorescence (TIRF) or förster resonance energy transfer (FRET) techniques has the capacity to increase resolution to only a few tens of nm (see below for more detailed information). Other techniques such as or narrowing the boundaries of the PSF by suppressing (de-

exciting) the fluorescence from the edge of the center spot of the airy pattern by e.g. stimulated emission depletion (STED), and other non-linear optical masking techniques have further enhanced optical resolution of confocal microscopes (Bullen 2008, Willig et al. 2006). However, these techniques are not yet compatible with fast scanning of Ca^{2+} events that take place over fast timescales, and will therefore not be discussed further here. Finally, secondary signal processing or deconvolution (which computationally reverses optical distortion to enhance resolution) also serve to enhance spatial resolution of both confocal and epifluorescence images by a further factor of 2-3.

Light scattering increases proportionally with specimen thickness, thus scattering becomes more of a problem with deeper imaging of thicker specimens. Therefore, appropriately setting the pinhole not only allows for imaging of thin optical sections, but also affects the signal-to-noise (SNR) ratio. Reducing the pinhole diameter increases XYZ-resolution (especially Z-, but also XY-resolution; see above) but reduces signal-to-noise ratio (SNR). Opening the pinhole to approximately match the projected image of the diffraction-limited spot ($1.22\ \lambda$ / NA, where λ is the illumination wavelength) will substantially increase the SNR with only minimal reduction in the Z-resolution (Conchello et al. 1994).

Limitations On Speed Of Confocal Imaging

There is always a trade-off between spatial and temporal resolution. The reason for the lower temporal resolution compared to widefield imaging is that conventional confocal imaging requires some form of scanning, i.e. sequential pixel sampling, in order to "build" an image, which thus happens pixel by pixel. In contrast, the whole field during widefield imaging is captured simultaneously either by PMTs or charge-coupled device (CCD) cameras (Ogden 1994). The removal of out-of-focus light allows for relatively fast imaging of ~0.6 μm thin sections either in spot, line, or frame modes that either may be repeated sequentially in time, or combined with stepwise up- or down-focusing through the specimen in order to generate 3D information. 3D sectioning does not allow for recording of cellular events in real-time, but repeated 1-dimensional (1D) line imaging or even repeated 2D imaging with reduced frame sizes or restricted pixel numbers in contrast do allow for relatively fast recording with a temporal resolution of approaching a μs scale. Although not as fast

as regular widefield imaging, even 2D frame imaging may still be acquired on fast time scales, usually within hundreds of ms, though there will be a trade-off between temporal and spatial resolution. For some Ca^{2+} events, imaging with a temporal resolution in the ms order may be satisfactory, but other events may occur much faster than this. Ultimately, the speed of confocal image acquisition depends on the mode and the settings of the scanning and how many pixels are scanned before returning to the same pixel again. This will be discussed later.

Laser Scanning Confocal Microscopy

Out-of-focus light rejection and image acquisition through a confocal aperture with a pinhole is the common principle that constitutes confocal microscopes, but the illumination and excitation principles may differ between various systems. First, confocal microscopy by laser scanning the specimen (laser scanning confocal microscopy, often abbreviated to LSM or LSCM) is the most widely used illumination and excitation method today.

During laser scanning confocal microscopy, a laser beam is directed on to the specimen. The scanned field may be a single spot (in reality rarely used for biological imaging apart from fluorescence recovery after photobleaching (FRAP) applications), a 1D line, or a 2D frame. The laser is controlled by the use of 2 oscillating mirrors in the scanhead that deflect the beam along a fast and slow axes perpendicular to one another. Thus, during a 2D frame scan, the beam is first directed along the horizontal axis, after which it "jumps" down one pixel and scans the next line, this process continues until a full frame has been scanned. This may then be repeated for serial frame scanning, or the plane of focus may be moved along the Z-axis for 3D imaging. The fluorescence emission returns along the same light path ("descanning"), but is deflected by a dichroic mirror that splits the excitation and emission lights, such that the emission light only is directed onto the confocal aperture, allowing in-focus light to reach the signal detector.

Unfortunately, scanning is the rate-limiting step in image acquisition because of the mechanical characteristics of the mirrors. A typical 512 x 512 pixel 2D frame may be scanned in ~1 s. Several approaches may be taken to increase scanning speed. One is to scan lines instead of frames, in this configuration the same line is scanned

sequentially for a given period of time to allow detection of one or more events occurring within the time frame of the scan. Although this provides a high temporal resolution, the acquired information is limited to a one-pixel wide area of the cell, such that events occurring elsewhere in the cell are missed. Furthermore, reducing the pixel dwell time (the period over which each pixel is scanned) also increases scan speed, but this also reduces the SNR. Reduced SNR may partially be compensated for by increasing the laser power, but this may exacerbate other problems such as photodamage to the specimen, especially in live cells, and photobleaching. In 2D mode, the size of the frame to be scanned may also be reduced, or fewer pixels may be scanned to yield the same speed up. The scan may also be run in a bidirectionally, though the two lines running in opposite directions may be slightly offset slightly blurring the signal. Several recent developments have increased scan speeds, in particular for 2D frame imaging, such as utilizing resonant oscillating mirrors in the scanhead instead of galvanometer-driven mechanical mirrors. Other developments include arranging prisms and acusto-optical deflectors into the excitation light path to illuminate the entire line simultaneously, instead of a pixel-by-pixel illumination applied by the conventional laser scanning microscopes described above. This means that the scanning in a 2D frame mode would only involve movement along one dimension (X), since the other dimension (Y) would all be scanned at once (simultaneously), and therefore, 2D frame scanning may be performed at linescan speeds or at speeds approaching video rates, if the emitted fluorescence is deflected onto a linear CCD cameraor PMT array. The disadvantage of these approaches is that true confocality will be lost because the pinhole of the confocal aperture must be replaced by one or more longitudinal slit openings to accommodate the simultaneous scanning of lines (hence, this is also called slit scanning). Finally, series of holographic or curved mirrors in the scan head have been used to scan more than one pixel at a time, but such technology is not in widespread use (Callamaras and Parker 1999, Tsien and Bacskai 1995).

The confocal scanning approaches discussed above use of single-photon lasers as the source of excitation. These are based on the principle that a single photon provides enough energy to excite a single fluorescent molecule, i.e. to “lift” it from a ground state to the excited state. The phase where the fluorophore is lifted to the excited state takes femtoseconds (10^{-15} s), the fluorophore remains in the higher-energy excited

state for picoseconds (10^{-12} s) it then undergoes internal conversion and starts to vibrate, which effectively leads to dissipation of energy, so that it drops back to the ground state with a time scale of nanoseconds (10^{-9} s). When this happens, the fluorophore releases a photon that, due of the loss of energy, has a longer wavelength (less energy), and this is what creates the fluorescence emission. The difference between the excitation and emission spectra (emission wavelengths being longer than excitation wavelengths) is called the Stoke's shift. The process of excitation and subsequent relaxation with fluorescence emission is illustrated in the Jablonski diagram (Figure 2) (and is not restricted to confocal microscopy, but is in fact the basis for all fluorescence techniques including epifluorescence microscopy and spectroscopy). As detailed above, it is the volume of the recorded fluorescent emission that differs between confocal and epifluorescence microscopy modalities. The volume of excitation may also differ, but this has to do with how much of the specimen is subjected to the illumination light. Although the laser excites fluorophores along the entire Z-axis of the specimen (see also above and figure 3), peak excitation and as such peak brightness occurs at the focal plane, whereas out-of-focus excitation decreases with the square of the distance from the focal plane. This is because the laser excitation beam presents with a bi-conical shape, with the intersection of the cone tips coinciding exactly with the focal plane.

Figure 2.

Several types of lasers have been developed that ensure single-photon excitation of fluorescent Ca^{2+} indicators (fluorophores), in particular the multi-line argon ion (Ar-ion) laser that provides high-intensity light from ultraviolet (UV) to the green wavelengths (~250 nm to 514 nm); the single-line helium-neon (He-Ne) lasers that extends the covered spectrum to ~633 nm, and argon-krypton (Ar-Kr) lasers that provide high-intensity light from blue to red wavelengths. Recent developments in solid state and diode lasers have added further choices to the microscopist.

Total Internal Reflection Fluorescence (TIRF) Microscopy

Confocal microscopy coupled to TIRF provides a very thin optical section of fluorescence excitation that allows imaging with low background noise and minimal out-of-focus fluorescence. This is because total internal reflection can occur when the

excitation light beam in a medium of high refractive index reaches an interface of a medium with a lower refractive index at an angle of incidence that is greater than the specific critical angle θ. When the light is totally internally reflected, none of it penetrates the medium with the lower refractive index, and (ideally, at least), there is no net energy flux escaping the glass. However, the reflected light generates an electromagnetic field that penetrates beyond the interface and into the lower-refractive index medium as an evanescent wave. This wave has a wavelength similar to the excitation light beam, and decreases in intensity exponentially with the distance into the medium. The penetration depth of the evanescent wave may be manipulated by changing the angle of incidence beyond the critical angle, which thus may be calculated accurately by knowing the angle of incidence, but will typically be limited to ~100 nm or less (Cleemann et al. 1997, Mashanov et al. 2003). This allows imaging of Ca^{2+} events occurring in close proximity to the plasma membrane of live cells. The limitation of this technique is that the cell must be positioned within the evanescent wave and not above it on the glass surface, which is possible if the cell is over a certain size and/or has a non-uniform morphology. In our experience, it requires an experimental effort to physically position large cells such as e.g. cardiac muscle cells with typical dimensions of 120 · 25 · 20 μm within the evanescent wave and yet still maintain physiological conditions for the cell. This is required because the evanescent wave is generated from the glass surface and not from the boundary of the cell.

Figure 3.

Förster Resonance Energy Transfer (FRET) Microscopy

Confocal microscopy coupled with FRET imaging to measure Ca^{2+} has experienced something of a surge of interest, because of the development of Ca^{2+}-sensitive cameleons. The FRET process is based on non-radiative energy transfer from a fluorophore in an excited state ("donor") to another chromophore ("acceptor") that usually is (but does not have to be) a different fluorescent molecule (fluorophore) within a range of 10-100 Angstroms (1-10 nm) (Jares-Erijman and Jovin 2003). Thus, when FRET occurs, it is not only the acceptor emission that will be recordable, but the measurable emission from the donor will also be greatly reduced because of the energy transfer. The intensity of the two emission bands depends on the distance between the two donor and acceptor fluorescent proteins or molecules even within the

FRET distance; the closer the distance between the donor and acceptor, the greater the longer-wavelength emission (from the acceptor) and the less the shorter-wavelength emission (from the donor). The fluorescence emission from the acceptor is discernible from the donor emission due to the spectral redshift, such that the instrumental requirement is that the two emission bands must be separately recordable. The presence of the longer-wavelength acceptor emission will confirm that the acceptor molecule is within the FRET distance of the donor, i.e. within a distance of ~10 nm. Likewise, the absence of it suggests that the physical distance between the donor and acceptor is larger than that. Traditionally, FRET imaging has been used to study protein-protein interactions by tagging different proteins with fluorescent probes, e.g. yellow or green fluorescent proteins (GFP) and thereby study whether they exists inside or outside the FRET distance.

The recent development of cameleons has made FRET imaging useful in studies of Ca^{2+}. Cameleons are genetically encoded fluorescent proteins that are sensitive to Ca^{2+}, in which a blue- or cyan-mutant of GFP (serving as the donor), calmodulin that can bind to Ca^{2+}, a calmodulin-binding peptide such as the calmodulin-binding domain of skeletal muscle myosin light chain kinase (the M13 peptide), and a long-wavelength yellow-mutant or normal GFP (serving as the acceptor) are tandemly fused (Miyawaki et al. 1997). This configuration forms a stable and compact complex that remains intact once transfected into the target cell. Subsequent development has improved the spectral properties and rendered the cameleons less susceptible for changes in e.g. pH (enhanced GFPs). In the absence of Ca^{2+}, the cameleon remains in its linear tandem configuration, whereby the two GFP mutants (donor and acceptor) at the two flanks of the tandem are too far apart to create FRET. However, when the concentration of free Ca^{2+} increases, calmodulin binds to Ca^{2+} and undergoes a conformational change that also leads it to wrap around the M13 peptide, creating a compact configuration of the cameleon that brings the donor and acceptor GFP mutants to within a distance where energy transfer may occur with much greater efficiency. Thus, the presence of Ca^{2+} creates FRET by the cameleon, which may be readily detected. Because Ca^{2+} affinity can be tuned by incorporating mutations into the calmodulin protein, cameleons may detect free Ca^{2+} concentrations in the range 10 nM to 10 mM, and this has been done to visualize local Ca^{2+} signals in the nucleus, sarco/endoplasmic reticulum, and the cytosol, by transfecting chimeras of the

cameleon that also have the appropriate localization signals encoded in the complementary DNA (Miyawaki et al. 1997). A typical example of a cameleon used for FRET imaging of Ca^{2+} has an excitation spectrum peak at 442 nm for the donor (blue-mutant of GFP), with the associated emission peaking at 486 nm. This wavelength FRET-excites the GFP on the acceptor side, which then emits longer wavelength fluorescence with a peak at 530 nm (Figure 4).

Figure 4.

Several protocols for detecting and measuring FRET efficiency have been developed, some of which are applicable to imaging of Ca^{2+} signals. These include measuring donor quenching, i.e. measuring the decrease in the emission from the donor fluorophore, which appears because some of the energy emitted by the donor fluorophore is used to excite the acceptor chromophore/fluorophore. This is done by taking the ratio between donor and acceptor fluorescence during FRET as the numerator, and the same ratio in the absence of FRET (i.e. by removing either of the donor or acceptor fluorophores) as the denominator. As with all ratiometric quantifications, this has the advantage that the measure becomes independent of local variations in fluorescence; whereas the disadvantage is that both the donor and acceptor fluorophores may be quenched by other factors that would distort the results. Another method for measuring FRET efficiency is by measuring donor quenching and acceptor photobleaching, i.e. the intensity of the donor emission in the presence of an acceptor relative to the intensity of the donor emission in the absence of an acceptor. In practice, the latter is done by first photobleaching the acceptor by illuminating it with light at the peak excitation spectrum of the acceptor fluorophore, before measuring the donor emission. This protocol is made possible by photobleaching itself causing the fluorophores to loose their ability to fluoresce. However, because photobleaching may take up to 20 minutes to achieve, this may be unsuitable for use with live specimens. Finally, FRET combined with fluorescence lifetime imaging (FLIM) has introduced a robust option for Ca^{2+} measurements, because it largely is unaffected by experimental conditions such as fluorophore concentrations and excitation intensities. In this combined FRET-FLIM approach, the change in donor lifetime is measured in the presence and absence of an acceptor. The principle behind this is that the period of time the donor will fluoresce (i.e. the lifetime of the donor)

depends on the presence or absence of an acceptor (Levitt et al. 2009). As described above, the measurement of donor emission in the absence of an acceptor may be done by first photobleaching the acceptor. However, once the photobleached control images have been captured, this protocol allows for detailed imaging of Ca^{2+} signals.

Since the introduction of cameleons, derivatives have been developed that fuse Cam with the Cam-binding peptide M13 in a similar fashion as cameleons, but are based on single GFPs instead of two GFP mutants with different spectral properties that necessitate Ca^{2+} imaging by FRET. These derivatives, called pericams, can therefore be imaged by standard epifluorescence or confocal microscopes, and present with broad Ca^{2+} sensitivities and different localization sequences that allow for measurements of a range of Ca^{2+} concentrations within specific organelles and intracellular targets (Kettlewell et al. 2009, Nagai et al. 2001).

Parallel Scanning Confocal Systems

The main limitation of the traditional laser scanning confocal microscope systems discussed so far is their low full frame temporal resolution. Typical rates of just a few frames per second are one-two orders of magnitude slower than necessary to follow the fast Ca^{2+} dynamics of systems such as neuronal networks or cardiac and muscle tissues.

Recent developments in parallel multi-spot confocal illumination devices have gone some way to addressing these concerns, providing high contrast optical sectioning with typical rates in the 10-100 Hz domain. Multi-spot systems use an aperture mask at an illumination plane conjugate with the sample, where multiple illumination points with non-overlapping airy disk profiles are projected to the sample simultaneously. This illumination pattern is then changed in a sequential fashion such that every image point is uniformly illuminated in a given time interval. The parallel illumination approach has the obvious advantage that all image points can be illuminated much faster than in a conventional single scan system, but it requires a 2D imaging detector to record the image, which then becomes the limiting factor for capturing image frames. Limitations of the detectors (typically CCD cameras) are further exacerbated by the requirement for fast detection, as these devices have a noise floor below which the fluorescence signal cannot be resolved. The fundamental problem is that in order

to increase frame rates, the exposure time of a frame must be reduced, thus limiting the number of detectable photons in the integration interval. Simultaneously, the transfer rate of data from the camera has to be increased; a process which increases read noise of CCD cameras increases. Many of these concerns are resolved by modern high-end electron multiplication (EM) CCD cameras such as the iXon 897 (Andor), Evolve (Photometrics), or ImagEM (Hamamatsu). These EM-CCD cameras can amplify small photoelectron signals above the read noise of the camera; providing the sensitivity and speed required to make these theoretical parallel approaches a practical reality.

Two approaches used to achieve this fast pattern change are (i) the Nipkow spinning disk where a patterned disk is spun at high speeds, and (ii) programmable matrix systems (digital mirror and liquid crystal arrays) where individual pixels can be switched “on” and “off” very fast.

Spinning Disk Confocal Microscopy

These systems illuminate the specimen simultaneously with multiple non-overlapping points of light by using hundreds to thousands of pinholes arranged in a geometrically precise spiral pattern on a spinning disk (Nipkow disk). The disk is placed at an image plane conjugate with the sample, and the illumination is filtered by this disk. Thus, the specimen is raster scanned rather than single-spot scanned (such that the entire 2D frame may be illuminated semi-simultaneously). Fluorescence emitted from each illumination point then returns through the same aperture of the mask to give a set of confocal points in the image. When the disk is spun at high speed (typically several thousand revolutions per minute), an apparently continuous image is obtained when viewed through an eyepiece. The resultant image is traversed with scan lines, but precise synchronization of the illumination and detection systems virtually eliminates this artifact in well configured systems (Wilson et al. 1996). This approach allows for very fast scan rates without significantly compromising the SNR (Wang et al. 2005).

As the input illumination power is spread over a much larger area than with conventional scanning confocal systems, light throughput can be a serious impediment to successful implementation of spinning disk systems. This was partially resolved by enhancing the original design by means of a second disk spinning in

sequence with the Nipkow pinhole array disk. This second disk is sited between the dichroic and the light source and contains a microlens array that maps a miniature lens to each pinhole (Tanaami et al. 2002), thus improving the illumination efficiency by focusing the lightbeam onto the pinhole (Figure 5A). This also reduces the backscattering of light at the surface of the Nipkow disk, which substantially increases SNR. The emission detection pathway is not affected by this modification. Use of specialist intensified cameras and fast versions of the spinning disk head can now enable imaging rates of up to 2 kHz. However, the drawbacks are that the pinholes on the spinning disk are inflexible, and the dwell time per pixel is usually very short (~100 ns), which may severely reduce the SNR, although the frequent illumination of the same pixel as the disk rotates may compensate for this.

Figure 5.

Programmable Matrix Microscopy

These instruments are based on the principle of spatially filtering full field illumination in a defined pattern at high speed, so as to give it a prescribed, dynamic structure. By using appropriate filtering patterns, the device can simulate the optical behaviour of confocal scanning microscopes. These systems are directly comparable to the spinning disk approach in that the illumination device consists of an array of small apertures that act as both the illumination and detection pinholes. The principal difference, and advantage, is that the elements of the array are individually addressable, allowing far greater flexibility in experimental design compared to the spinning disk (Hanley et al. 1999). For example, selectively and sequentially illuminating individual cells within the field is possible with the array system, whereas the Nipkow disk can only operate at full frame.

Two technologies have been used in implementing practical programmable matrix systems. The first makes use of a digital micro-mirror device (DMD), an array of micrometer-sized mirrors whose angle can be independently controlled to direct illumination to an “on” (confocal) or “off” pathway. The alternative uses a reflective liquid crystal display (LCD), an array of μm-sized liquid crystal ‘pixels’, the base of which is coated with a reflective layer (Figure 5B). Each element is individually addressable, creating a controlled polarization pattern that is optically transformed

into a confocal intensity pattern. So far, the liquid crystal approach forms the basis for the commercial utilization of this technique. This allows for using both the confocal image (conjugate with the array mask) and non-conjugate image to provide further potential enhancements in dynamic image quality (Heintzmann et al. 2003).

The real power of the programmable matrix approach lies in the ability to redefine the array composition, without any additional hardware changes. This enables complete flexibility for optimization of the illumination pattern for the sample and experiments in hand – from low speed high resolution to high speed lower resolution studies.

Advantages And Disadvantages Of Confocal Microscopy

From an experimental point of view, confocal Ca^{2+} imaging offers many benefits over conventional fluorescence microscopy, especially with respect to spatial and temporal resolution and the ability to optically section the specimen along the Z-axis down to a resolution of 0.5-1 μm, enabled by the presence of confocal apertures with pinholes in the light path that effectively gives this imaging modality its uniqueness, as well as its name. Importantly, confocal microscopy does not impair the ability to manipulate the surrounding environment in terms of solutions in which the cells or specimen are bathed, solution pens, temperature devices, application of pharmacological drugs and inhibitors, patch pipettes, electrical and mechanical manipulators, etc, as long as these do not interfere with light pathways. However, the significant drawbacks with confocal microscopy relate firstly to the unavoidable scattering as well as chromatic aberration with subsequent focal plane offsetting that reduces confocal signal collection of the illumination light as it penetrates the specimen (Bliton et al. 1993), especially as the wavelengths of ~300-600 nm commonly used for excitation are very prone to scattering, effectively limiting the penetration depth to ~40-50 μm (or less, depending on the laser output and the spectral properties of the specimen). Also, although only the emitted fluorescence produced at the or very near to the focal point is recorded, excitation still occurs along the whole Z-axis of the specimen (given molecules able to be excited are present along the Z-axis). This presents often considerable problems because the photodamage generated along the entire Z-axis may kill live specimens. Moreover, the restricted light capturing from the small volume accommodated by the pinhole tends to drive toward microscopists increasing rather than reducing laser power. This is especially true at short, including UV,

wavelengths (300-500 nm), as those are most severely damaging to live specimens. Finally, these systems have higher purchase and maintenance costs relative to conventional epifluorescence and widefield microscopes.

Multiphoton Excitation Laser Scanning Microscopy

A conceptually different approach that also allows optical sectioning and high spatial and temporal resolution live specimen imaging, and that also comes with other added benefits, is multiphoton microscopy. From a biophysical perspective, multiphoton imaging relies on excitation of the fluorescent molecule by photons that alone do not have enough energy, but need to combine by simultaneously coming in to a very close proximity of the fluorophore.

Although the theory of multiphoton excitation is relatively simple and has been known and used by physicists for many decades, biological applications of multiphoton excitation are much more recent (Denk et al. 1990). In confocal single-photon laser illumination, the fluorophore is excited by the absorption of a single photon, as it provides sufficient energy for the fluorophore to reach an excited state. Upon return to the ground state, a photon of longer wavelength than the excitation photon is emitted, creating fluorescence. With multiphoton excitation, a fluorophore is excited by the near-simultaneous (within 10^{-18} s) absorption of two or more photons that combined provide enough energy to promote the fluorescent molecule from a ground state to an excited state. Two-photon (2P) excitation is by far the most common multiphoton excitation modality. Thus, with 2P excitation, the fluorophore absorbs two photons simultaneously, each twice the wavelength and half the energy required for molecular excitation, and likewise, in three-photon (3P) excitation, each of the three excitation photons have three times the wavelength, but only one third of the energy compared to single photon excitation (Helmchen and Denk 2005).

Following 2P excitation, the emitted fluorescence is proportional to the square of the excitation intensity (measured in Goppert-Meyer units). This excitation occurs only at the focal point, as it is only here that the density of the excitation photons is high enough to ensure simultaneous photon arrival at the fluorophore. Though this may not occur with all photons in the volume, the probability of it occurring for the vast majority of the photons is very high. This non-linear excitation constitutes the most

important physical difference from confocal single-photon excitation, in that excitation will be confined to a small ellipsoid volume around the focal point, while above and below this point, the density of photons is not high enough to generate any excitation (Figure 6). This effectively means that out-of-focus fluorescence will not be generated, removing the need for a confocal aperture with a pinhole in the emission light pathway. The spatial resolution achieved is as good as, or almost as god as, that achieved by confocal microscopy at comparable temporal resolution (Cox and Sheppard 2004). A clear benefit of this is that there need not be a confocal aperture. Removing the confocal aperture means that the emitted fluorescence may be focused directly onto a PMT without having to be descanned. Consequently, 2P microscope systems are generally more light sensitive. However, a confocal aperture with a pinhole may optionally be introduced into the 2P emission pathway to improve the spatial resolution to a single-photon confocal standard.

Figure 6.

Although the capture of the emitted fluorescence involves different light paths in 2P excitation microscopy, it is similar to single-photon microscopes in that emission light needs be split from the excitation light with the insertion of an appropriate dichroic mirror. In the case of 2P microscopy, the emitted fluorescence will in most cases have a very much shorter wavelength than the excitation wavelength.

2P excitation offers several important advantages. First, because light scattering declines steeply with increasing wavelengths, red and IR (670 – 1100 nm) light will penetrate and hence excite fluorescent molecules much deeper into the specimen than single-photon lasers providing excitation wavelengths in the range from ~300 to ~600 nm. With sufficient power output and optimized optics including corrective optics for pulse dispersion, penetration depths approaching 1000 μm (1 mm) may be achieved, which considerably exceeds the ~40-50 μm achievable by single-photon excitation microscopes. To achieve ~20-fold deeper imaging with single-photon confocal microscopy, tissue or layer removal with histologic techniques or penetration by the objective would have been required. Such approaches are obviously unsuitable for live tissue. For this reason, confocal microscopy is mainly restricted to studies of single, isolated cells or tissue surfaces, whereas 2P excitation laser scanning

microscopy allows deep tissue imaging, including that of intact organs. For this reason, 2P excitation microscopes are typically more often upright rather than inverted, to allow tissue preparations to be set up on the stage, whereupon the objective lens is lowered to within the optical range for imaging. Even with 2P excitation deep tissue imaging, one can be assured that the vast majority of the fluorescence comes from the focal point and not from residual scattering (scattering is greatly reduced, but not obliterated, by long-wavelength excitation). This is because, even in strongly scattering tissue such as e.g. the heart, the density of scattering exciting photons is too low to generate any significant fluorescence. It should however be noted that penetration depths also heavily depend on the specimen, as different tissue properties may degrade the illumination as well as the emitted fluorescent light. In particular, tissues rich in collagen and myelin are known to be susceptible to this problem (Helmchen and Denk 2005).

Another advantage of 2P excitation is that IR light is much less phototoxic and photodamaging than shorter wavelengths. Also, because of the non-linear excitation, photodamage and bleaching are restricted to the focal point. Importantly, the reduced photodamage and fluorophore bleaching permit longer imaging periods.

2P excitation spectra of most fluorophores are broader than the equivalent single-photon excitation spectra, whereas the associated emission spectra after 2P and single-photon excitation are similar. This means that the same excitation wavelength may potentially excite several fluorophores with distinct emission spectra (Bestvater et al. 2002, Xu et al. 1996). This useful property will be explored in more detail later in the chapter. Moreover, whereas the positioning of the confocal apertures relative to the light detector as well as the focal plane is critical to ensure that the images of the source and detector apertures are cofocused, this is not the case for 2P excitation microscopes because fluorescence emission will only be generated at and tightly around the focal volume.

However, 2P excitation is not without problems. First, 2P excitation requires very high light intensities - intensities that would instantly vaporize the specimen if the light were delivered continuously. This is overcome by using lasers that provide ultrabrief (10^{-13} s) pulses at very high frequencies (~80-100 MHz), thereby generating

very high instantaneous energy, but sufficiently low average energy to avoid substantial damage to the specimen. Thus, the distance between each pulse is typically ~10 ns, whereas the width of each pulse itself is typically 100 fs (Figure 6). The high repetition rates match fluorescence lifetimes closely (see above) such that a good balance between excitation efficiency and onset of saturation is achieved (Helmchen and Denk 2005). The most widely used lasers that fulfil this criterion and provide the necessary wavelengths, are the solid state titanium:sapphire (Ti:Sapphire) oscillating (pulsed) lasers. These lasers are tunable, such that the latest versions are capable of delivering wavelengths in the range ~670 to 1100 nm; thus, from visible red to infrared (IR). This range is progressively expanding, as is power output by manufacturers. Though most 2P excitation applications may not be power-limited, more available power does benefit applications requiring deep tissue penetration. Typical power outputs in the latest Ti:Sapphire lasers may exceed 4 W at 800 nm, though the microscope optics may not be optimized for IR light and may cause a major loss in power from the outlet of the laser to the focal point of the objective lens. Glass components of the optical pathway also cause a dispersion (spreading) of the ~100 fs laser pulses, but this may be compensated for by corrective optics in order to maximize 2P excitation (Diels et al. 1985). Another limitation of 2P excitation microscopy is that reflected light imaging is not possible and it is not suitable for imaging highly pigmented specimens that absorb IR and near-IR light.

Ca^{2+} Indicators For Use In Confocal And Multiphoton Microscopy

For many years, biology has benefited from the fluorescent dyes or constructs that bind and therefore can measure the free concentration of Ca^{2+} [Ca^{2+}]. These indicators have been used to examine the levels and time course of changes in [Ca^{2+}] within the cytosol and the various organelles within the cell (e.g. nucleus, mitochondria, sarco/endoplasmic reticulum). The two main categories of indicators used for this purpose are small synthetic organic molecules based on the fast Ca^{2+} buffer BAPTA (Tsien 1980) or modified versions of natural Ca^{2+} binding proteins (Miyawaki et al. 2003). Both categories "sense" Ca^{2+} by chelating the ion which changes the structure/chemical properties of the ligands. Several modes of fluorescence have been utilized to report Ca^{2+} (summarized in Figure 7).

Figure 7.

Absorbance/quantum yield. In this case Ca^{2+} binding causes a change in the intensity of the fluorescence from the dye; typically Ca^{2+} binding causes an increase in fluorescence (Figure 7A). This mode is the most common employed by the fluorescent Ca^{2+} indicators used in confocal or 2P microscopy. In particular Fluo-3, Fluo-4 and Oregon Green all show dramatic increases in fluorescence upon binding to Ca^{2+}, while Fura-Red fluorescence decreases upon Ca^{2+} binding. The optical arrangement required for these dyes is the simplest, i.e. single excitation and emission wavelengths.

Spectral shift. In this case Ca^{2+} binding causes a shift in either the excitation or emission wavelengths. Fura-2, and related dyes show a shift in the excitation spectrum of the dye with minimal changes in the emission (Figure 7B). In contrast Indo-1 and related dyes show large shifts in the emission spectrum of the dye with minimal changes in the excitation spectrum. This spectral shift allows ratiometric measurements of Ca^{2+}. In the case of Fura-based dyes, while exciting at ~340 nm, a rise of Ca^{2+} will cause an increase in fluorescence; whereas exciting at 380 nm, it causes a decrease. The ratio of fluorescence at these two wavelengths is a function of $[Ca^{2+}]$ that is independent of the concentration of the dye. This is particularly useful when measuring cells that move and so alter the amount of dye within the light path, or when comparing cell compartments with different dye concentrations (e.g. nucleus versus the cytosol). However, despite all these advantages, the Fura- and Indo-based dyes are rarely used in confocal microscopy because excitation wavelengths are short (<400 nm) and therefore not convenient for commonly available lasers. The shortest wavelength routinely available in commercial systems is 405 nm, which can be used to excite Fura-based dyes close to the 380nm excitation maximal. In this mode, Fura acts as an inverse indicator, a property that has some value in single-photon confocal and 2P imaging (Ogden et al. 1995, Wokosin et al. 2004).

Fluorescence lifetime. In this case, the decay of fluorescence at the end of a pulse of excitation light will take a finite time (ns). The time course of decay is affected by the binding of Ca^{2+} (Figure 7C). In the case of Fluo-3, the decay of fluorescence or lifetime is shorter for the Ca^{2+} bound form (Sanders et al. 1995). Since the lifetime is independent of the concentration of the dye, the relative population of bound and free

dye can easily be calculated from this technique. However, the non-trivial analysis of emission decay required to obtain lifetime data has minimized the use of this technique.

Förster resonance energy transfer (FRET) Efficiency. In this case a donor molecule absorbs photons and can transfer the associated energy to a nearby acceptor molecule via a non-radiative process that operates at distances less than the wavelength of light (up to 10 nm). The closely adjacent molecule accepts the energy transfer (thus excites) and then emits light at a distinct wavelength (Figure 7D). The most popular pairs of donor and acceptor molecules are cyan fluorescent proteins (donor) and yellow fluorescent proteins (acceptor). The efficiency of the energy transfer depends on the proximity of the two molecules; within 10 nm, the efficiency is high but this drops dramatically as the distance between the two molecules increases (proportional to $1/\text{distance}^6$). This mechanism can be used to detect Ca^{2+} binding to either construct since the change in tertiary structure will change FRET efficiency and therefore modulate the FRET signal.

Use Of Dyes For Single-Photon Confocal Microscopy

In theory, all the fluorescent Ca^{2+} indicators created for cell biology can be used in confocal or 2P excitation modes, although in practice only a limited number of dyes are routinely used, for a number of practical reasons. By far the majority of confocal applications use single-wavelength excitation and emission dyes. These dyes have several advantages: (i) their excitation wavelength is ~500 nm or longer and therefore can use the emission from readily available Argon or Krypton Argon lasers, and (ii) the majority of dyes have a good dynamic range (see below). However, they also suffer from some disadvantages: (i) calibration is difficult because the signal is a function of both the concentration of the dye (unknown and variable) and the concentration of Ca^{2+}, and (ii) dye signal may vary over time due to loss of the dye from the volume or due to photo-bleaching. All dyes photobleach, but some dyes are more susceptible than others; Fluo-3 and Fluo-4 are amongst those that most rapidly bleach (Thomas et al. 2000). Dyes that show significant spectral shifts can be used in a single wavelength mode, for example Fura-based dyes can be imaged in confocal microscopy by using a 405 nm laser. This produces an inverted signal since fluorescence decreases as Ca^{2+} increases (Wokosin et al. 2004). Similar measurements

using Indo-based dyes are harder because the narrow excitation spectrum means that 405 nm laser light only poorly excites the dye, and Indo-based dyes appear to be inherently more prone to photobleaching.

Use Of Dyes For 2P Excitation Microscopy

The utility of a dye for imaging Ca^{2+} using 2P excitation does not follow directly on from the behaviour of the dye to single-photon excitation. There is no guarantee that 2P excitation will successfully excite the dye since the efficiency of two photon excitation appears to be relative to the fluorophore structure (Kim et al. 2008). A number of Ca-sensitive indicators have been studied over a limited range of 2P wavelengths (Xu et al. 1996). Some dyes (e.g. Oregon Green) have a better 2P cross-section than the more common single wavelength dyes (Fluo-3); none showed the expected increase in cross-section as the excitation wavelength approached 900 nm. In contrast, the 2P cross-section of Fura-based dyes appeared readily excitable by wavelengths approximately double the appropriate single-photon wavelength (Wokosin et al. 2004). In particular, ~800 nm light provides an inverse Ca^{2+}-sensitive signal that correspond to the excitation of this dye at ~400 nm, as advocated previously (Ogden et al. 1995). However, few studies to date have explored the more commonly used dyes (Fluo-3/4 and Rhod-2) at the longer wavelengths achievable currently with tunable Ti:Sapphire lasers (up to 1100 nm). As shown in Figure 8, the Fluo-based dyes do not show the peak of fluorescence anticipated from approximately double single-photon wavelengths (~1000 nm). The small peaks in the excitation spectrum observed at 400-470 nm during single-photon excitation were also paralleled by similar spectra at 800-950 nm during 2P excitation, but longer wavelengths failed to produce the increased fluorescence anticipated from the single-photon spectrum. The behaviour of the Rhod-dyes (related structurally to Fluo-dyes) has yet to be examined in detail mainly because accessing wavelengths >1100 nm is technically difficult. The practical application of 2P excitation to excite Ca^{2+}-sensitive dyes is limited; the majority of applications used ~800 nm to excite either Fluo-3 or Rhod-2. In doing so, these studies are using the higher powers available from lasers at these wavelengths, rather than attempting to access the higher quantum yields that may be present at longer wavelengths. Further work is required to examine the optimal 2P conditions required to excite these readily available dyes at 1000-1100 nm,

or alternatively design new dyes with fluorophore structures that are more easily excited by the 2P approach (Kim et al. 2008).

Figure 8.

Is It Worth Converting The Intracellular Fluorescence Signal To [Ca^{2+}]?

Ca^{2+}-sensitive dyes are frequently used in conjunction with confocal microscopy to simply indicate the timing or frequency of transient Ca^{2+} events. Under these circumstances it is not considered necessary to convert the fluorescence signal into estimates of intracellular [Ca^{2+}]. This is partly for experimental ease, since conversion requires knowledge of the concentration of the dye and its affinity for Ca^{2+}, and partly because absolute Ca^{2+} concentrations are not considered vital to the interpretation of the experiments. In a number of cases this may be justified, but whenever amplitude or time course of a Ca^{2+} transient is considered an important variable, then calibration becomes essential for two reasons:

1. It is important to distinguish changes in background Ca^{2+} from one experimental scenario to the next since this determines the subsequent intracellular Ca^{2+} buffer power. Any event that generates a Ca^{2+} transient, e.g. Ca^{2+} influx via plasmalemmal Ca^{2+} channels or Ca^{2+} release from an internal store, will increase total intracellular Ca^{2+} by a specific amount, but the extent to which this increases the free cytosolic Ca^{2+} concentration will depend on the cellular buffer power for Ca^{2+}. This is illustrated in Figure 9. When total cellular Ca^{2+} is increased by a standard amount, the subsequent free Ca^{2+} transient amplitude can be ~40% larger simply because of small (~10%) changes in resting [Ca^{2+}]. Therefore, if the basal Ca^{2+} concentration changes, any changes in transient amplitude have to be interpreted with caution.
2. Intracellular [Ca^{2+}] levels that almost saturate the indicator cannot be used to examine moderate changes in the amplitude of the Ca^{2+} transient. In the absence of information concerning the maximal Ca^{2+} signal, it is difficult to know how close the dye is to saturation and therefore how sensitive the signal is to changes in peak Ca^{2+} level.

Figure 9.

Calibration Of Single Wavelength Dyes

Calibration of single wavelength dyes is based on two main assumptions; firstly, that the dye is at equilibrium with intracellular Ca^{2+}, i.e. the kinetics of the change of intracellular Ca^{2+} are slow compared to the rate constants for association and dissociation. For the commonly used Fluo-type dyes at intracellular concentrations of <100 μM, the half-times for association and dissociation are of the order of ~1 ms and therefore for most circumstances the equilibration assumption holds. The second assumption is that all the dye molecules sense the same amount of light, i.e. there is no filtering intrinsic to the biological preparation or by the dye itself. Typically, the absorption coefficient of Ca^{2+} indicators is of the order of 50,000 $M^{-1} \cdot cm^{-1}$, therefore significant absorbance (>0.05) would occur in a cell 10 μm thick containing >100 μM dye. This consideration is important for single-photon excitation, and is one of the constraints that limit single-photon imaging to thin (<50 μm) specimens.

When these two criteria are satisfied, the Ca^{2+} concentration can be calculated from the fluorescence from single wavelength dyes using the following equation:

$$[Ca^{2+}] = K_d \cdot (F-F_{min})/(F_{max}-F)$$

where F is the fluorescence signal from the cell/tissue, K_d is the dissociation constant of Ca^{2+} for the indicator (units M), F_{min} is the minimum fluorescence achieved when the dye is essentially Ca^{2+} free, which practically can be approximated by exposing the dye to a $[Ca^{2+}]$ that is $0.01 \cdot K_d$ of the dye, and F_{max} is the fluorescence achieved when the dye is completely Ca^{2+} bound, which practically can be achieved with $[Ca^{2+}]$ of $100 \cdot K_d$ of the dye. Measurements of these constants with a high degree of precision inside a cell are nonetheless difficult. The dissociation constant can be measured outside the cell in solutions approximating the intracellular mileau, but it has been a frequent observation that the value of the K_d is altered by the intracellular environment in a way that is difficult to mimic by solution chemistry, e.g. mimicking intracellular viscosity and the range of negatively charged intracellular proteins (Poenie 1990). Therefore, the best practice is to measure the dissociation constant within the cell type of interest. The easiest way to achieve this is by using a glass microelectrode to gain access to the intracellular space. The use of a series of solutions with a high concentration of Ca^{2+} buffer (EGTA or BAPTA) with specific

$[Ca^{2+}]$ can be used to make a series of single cell measurements to allow estimation of K_d. It is important to note that this technique cannot be applied to multicellular preparations where multiple cells in a tissue are differentially loaded with the dye.

Estimation Of F_{max} values

This should be measured on a cell-to-cell basis even in multicellular preparations and involves exposing the inside of the cell to ~50 μM or higher Ca^{2+}, depending on the affinity of the dye for Ca^{2+}. These levels are generally toxic to cells, but if tolerated for a short time (1-2 s); this may be sufficient to estimate F_{max}. These intracellular $[Ca^{2+}]$ levels can be achieved rapidly within single cells by perfusion with a Ca^{2+} ionophore and raised extracellular Ca^{2+} (Loughrey et al. 2003). A second ingenious method used in single voltage clamp experiments is to use an amphotericin-containing patch pipette that facilitates monovalent cation exchange across the membrane within the patch and therefore allows low resistance access to the cell. At the end of the experiment, the membrane is ruptured under the patch using a rapid pressure step and the resultant influx of Ca^{2+} from the patch pipette generates a rapid rise of intracellular $[Ca^{2+}]$ that can be used to assess F_{max} (Diaz et al. 2001). A simpler but less reliable method is to simply use the microelectrode to penetrate the cell and allow extracellular Ca^{2+} influx in order to record F_{max}, but generally Ca^{2+} influx occurs in parallel with a rapid loss of intracellular dye so the signals would have to be interpreted with caution.

Depending on the tissue, there are alternative approaches to estimation of F_{max}. In some nerve cells, rapid frequent stimulation of cells can generate intracellular Ca^{2+} levels that approach saturation of the dye (Maravall et al. 2000), thus allowing F_{max} values to be estimated.

Estimation Of F_{min} Or The Dynamic Range Of The Dye

Estimation of F_{min} or the dynamic range of the dye is a more difficult measure. The ratio of F_{max}/F_{min} measured outside the cell cannot be assumed to apply inside; estimates suggesting that values of ~70-80% of those seen in free solutions are common (Poenie 1990). Again, an average value can be obtained using patch pipettes as a means of establishing buffered $[Ca^{2+}]$ inside cells. Alternatively, the F_{min} in each experiment can be estimated if the intracellular Ca^{2+} can be lowered to 1-10 nM (for

Fluo-3) by decreasing extracellular Ca^{2+}, but this assumes that intracellular Ca^{2+} can be readily manipulated by changes in the extracellular environment which is not always the case for every cell type. The effect of under- or over-estimation of the dynamic range of the indicator is shown in Figure 10C. Based on the reported dynamic range of Fluo-based dyes (~100x), large under/over-estimates of the dynamic range (by up to 30%) cause only small errors in Ca^{2+} estimation, and only in the lower range of $[Ca^{2+}]$ values relative to the K_d of the dye.

Figure 10.

Consequence Of Errors In Estimation Of Intrinsic And Dye Fluorescence

Prior to conversion of the indicator-based fluorescence to $[Ca^{2+}]$, the background or intrinsic fluorescence of the cell/tissue has to be subtracted from the signal. All cells have an intrinsic fluorescence mainly due to the metabolites beta nicotinamide adenine dinucleotide (NADH) and flavin adenine dinucleotide (FAD); their excitation wavelengths are 350-500 nm and emission wavelengths ~450-600nm. The relative fluorescence of these two metabolites depends on the metabolic state of the cell/tissue and degree of photobleaching. Thus, intrinsic cellular fluorescence is significant and variable. The most advisable approach is to use a dye with a significant basal fluorescence that is many times (>10x) that of the intrinsic value. This cannot always be achieved; the Fluo-based and Rhodamine-based dyes are by far the most popular dye groups used in confocal and 2P excitation microscopy. Their main attraction is a large dynamic range as a result of a low fluorescence signal from the Ca^{2+} free form. In this situation, F_{min} values are frequently comparable to that of the intrinsic fluorescence of the cell and therefore it is important to quantify either by parallel measurements on non-loaded tissue or from a single cell prior to the introduction of the dye. Error in estimation of background fluorescence (which typically can be up to 100%) has dramatic effects on the calculation of intracellular $[Ca^{2+}]$ particular at either end of the sensitive range of the indicator at shown in Figure 10A. If the dye has a Ca^{2+} affinity midway between the extremes of intracellular Ca^{2+}, the error can be small and approximately constant. But if the dye has a lower Ca^{2+} affinity, which may be desirable to resolve changes in peak Ca^{2+}, then errors associated with the minimum cellular Ca^{2+} levels can be large.

These errors may be compounded by errors in estimates of fluorescence or the variability of signals from one cell to the next. Figure 10B shows the errors in Ca^{2+} based on simple errors in fluorescence changes. The graph illustrates the potential danger of using dyes with a relatively high affinity relative to the physiological signal. Small errors in the range of fluorescence signals translate to large errors of intracellular Ca^{2+} such that the ability to discriminate changes in maximum physiological response is severely impaired. This can be significantly improved by using lower affinity dyes, but at the cost of poor resolution of minimum or background intracellular [Ca^{2+}].

Multimodal And Multiple Fluorophore Confocal And Multiphoton Microscopy

Although Ca^{2+} is an important signaling molecule in a variety of cell types, it by no means operates alone. Rather, Ca^{2+} both temporally and spatially interacts with many other properties and processes in the cell that only together orchestrate cellular function. Thus, some of these processes are dictated by Ca^{2+}, but some are not. A good example of this interplay is the excitation-contraction coupling in muscle cells, in which an action potential depolarizes the plasma membrane of the cell, causing a small influx of Ca^{2+} through the membrane. This inward Ca^{2+} current stimulates the ryanodine receptor to release bulk Ca^{2+} from the sarcoplasmic reticulum, which upon binding to the myofilaments induces the actin-myosin interaction and the subsequent cellular contraction (Bers 2002). The cellular contraction may be imaged by simple black-and-white contrast edge-detection microscopy, but this is not the case for the intracellular Ca^{2+} and membrane potential characteristics that both require more sophisticated methods such as fluorescence microscopy. Thus, simultaneous imaging with the use of multiple fluorophores present at the same time in the specimen or combinations of different imaging modalities in some sense is required for capturing complex information.

For example, loading or injecting the specimen with multiple fluorophores allows for simultaneous recording of different signals; or if simultaneous recordings are not technically possible, different signals may be recorded sequentially without manipulating, moving, or in any other way perturbing the specimen between recordings. In the latter case, only the optical pathway of the microscope would be altered between recordings, whereas the specimen would not, since it would already

be loaded with different fluorophores. The use of multiple fluorophores requires either the ability to direct separate emission wavelength bands onto different light detectors, or to spectrally separate different fluorophores by excitation wavelengths. Depending on the hardware, both confocal and multiphoton microscopes can fulfill these requirements and therefore allow for measurements with multiple fluorophores. Such experiments can be done by simultaneously loading the specimen with e.g. a Ca^{2+}-sensitive fluorophore and a fluorophore that is sensitive for another characteristic of the cell, which may also be Ca^{2+} in a different compartment of the cell with different dynamics or a different concentration range, or e.g. a second fluorophore that may be sensitive to the plasma membrane voltage in an excitable cell (also called a potentiometric dye). Measurements of Ca^{2+} and membrane voltage (resting membrane potentials and action potentials) may then be conducted either simultaneously by exciting both fluorophores at the same time and capture spectrally different fluorescence emission signals, or sequentially by exciting each fluorophore separately, i.e. one after the other, under otherwise similar experimental conditions. The latter approach would assume that the experimental conditions remain the same. Several factors may necessitate this, such as an inability to differentiate between different emission signals, or an inability to excite more than one fluorophore at any given time, e.g. if the excitation spectra do not overlap and only one excitation wavelength may be delivered at any given time.

The advantage of using multiple fluorophores either simultaneously or sequentially is to increase the information content of the imaging, especially how different processes relate to each other spatially and temporally. However, several issues may limit the applicability of such measurements. Introducing a fluorophore to the specimen may also change the dynamics of the cellular parameter of interest, especially in live specimens that rely on stable and constant intra- and extracellular environments. For instance, most Ca^{2+} indicators are also Ca^{2+} chelators that buffer free Ca^{2+}, and most fluorophores or the medium they are delivered in may change biochemical and biophysical properties of the intracellular environment. This may be accentuated by simultaneous loading with several dyes. Different dyes may also quench, sequester, or in other ways inhibit each other. Finally, excitation in itself may cause changes or damage to the specimen, and although this to some degree is unavoidable, the degree

of change or damage may be different or even accentuated during sequential recordings.

The single-photon excitation and emission spectra of multiple Ca^{2+}- and voltage-sensitive fluorescent dyes are well-known. Clearly, some dyes have overlapping excitation or emission peaks, or present with broad excitation or emission spectra such that even if the peaks are separated from one another, the tails of the spectra still overlap considerably. Overlapping excitation spectra means that different dyes may be excited simultaneously, but overlapping emission spectra may result in severely reduced signal specificity, and therefore, certain combinations of fluorescent dyes may be less applicable, such as the potentiometric Di-4-ANEPPS and Di-8-ANEPPS dyes and the Ca^{2+}-sensitive Fluo-3 dye, all extensively used by numerous laboratories for single-fluorophore purposes. All of these dyes have single-photon excitation peaks at ~480-500 nm and emission peaks at 520-610 nm. Di-4-ANEPPS and Di-8-ANEPPS have very broad emission spectra that peak at ~610 nm, but that considerably overlap with the Fluo-3 emission spectrum, which peaks at ~525 nm and is narrower (Figure 11A). This problem may to some degree be avoided as the Ca^{2+} and voltage signals are spatially separated between intracellular and membrane compartments of the cell, though in muscle cells this may turn out to be difficult because of the dense network of plasma membrane transverse tubules that penetrate into the interior of the cell. The same overlap problem exists with the voltage-sensitive RH-237 and the Ca^{2+}-sensitive Rhod-2 dyes, with emission peaks occurring at ~580 and ~660 nm respectively, but with the RH-237 emission spectrum being very broad (Figure 11B). In contrast, Fluo-3 and RH-237 are more distinctly separated from one another. Both Fluo-3 and RH-237 dyes may be excited by the same single-photon excitation wavelength at ~500 nm (though RH-237 would not be optimally excited by this wavelength), but have emission spectra that may be spectrally differentiated, as Fluo-3 has a narrow emission spectrum that peaks at ~525 nm whereas RH-237 peaks at ~660 nm with a broad spectrum (Figure 11C). Thus, this combination appears attractive as it differentiates the Ca^{2+} and membrane potential signals (Fast and Ideker 2000).

Figure 11.

Several problems arise in going from single-photon to 2P excitation. Although the voltage-sensitive dyes present with consistent and reproducible 2P excitation spectra that closely resemble the doubled single-photon excitation spectra and may thus be reliably used for multiphoton imaging. In contrast, the 2P behaviour of many of the Ca^{2+}-sensitive dyes is less predictable and somewhat difficult to interpret (see previous discussion and Figure 8), though the ratiometric Fura dyes may be 2P excited in order to provide a meaningful Ca^{2+} signal that also captures transient changes over a ms scale with high fidelity (Wokosin et al. 2004). This may be because the Fura dyes have a single-photon excitation spectrum in the UV range (340 – 380 nm), and therefore the 2P excitation spectrum, which is approximately double the single-photon spectrum, peaks at ~800 nm wavelengths, in which the 2P laser power outputs are not limited. This study indicated that several of the Fura dyes, in particular Fura-4F, may work well when excited with a single IR wavelength, despite their use as ratiometric single-photon dyes, as judged by the dynamic ranges and SNR obtained during 2P excitation microscopy in single cardiac muscle cells during different Ca^{2+} conditions. In contrast, the Fluo- and Rhod-based Ca^{2+}-sensitive dyes, all with single-photon excitation peaks at ~500-550 nm, present with 2P excitation spectra that are not immediately predicted by the doubled single-photon spectra (Figure 8). In these cases, the 2P excitation spectra are at least partly broken up and appear blueshifted compared to the doubled single-photon spectra. Although doubling the single-photon excitation spectrum is often a good predictor for the 2P excitation spectrum, deviations from this do occur, and these deviations may not be systematic nor well understood (Xu et al. 1996, Zipfel et al. 2003). Furthermore, the available Ti:Sapphire pulsed 2P lasers are power-limited at the long wavelengths of 1000-1100 nm that would correspond to the doubled single-photon excitation spectra of Fluo-3 and Rhod-2. Therefore, because not all fluorophores translate easily from single-photon excitation, for which they were developed, to 2P excitation, the simultaneous use of multiple fluorophores for 2P excitation microscopy is problematic and remains to be fully resolved.

A different approach to capture more complex information has been to combine several multimodal microscopy techniques in ways that also encompass confocal and multiphoton systems, but also this comes with both advantages and disadvantages. For instance, different modes of contrast used on the same specimen may increase the

information extracted from the images and reduce artifacts. Multimodal microscopy may also allow for a wider repertoire of fluorophores. However, if confocal and multiphoton imaging are combined, it requires descanning and insertion of a confocal aperture with a pinhole into the light pathway, which may reduce the fluorescence capture after 2P excitation and thus lead to a loss of signal, though a confocal aperture may also be set up to increase the spatial resolution of multiphoton images, by restricting the PSF tails. Because of these limitations, the reality is often that it is difficult, though not impossible, to achieve optimal performance from each individual mode when several modes are combined. Nonetheless, the advantages of simultaneous or near-simultaneous light capture by different modes of microscopy may under the right circumstances far outweigh the disadvantages.

Examples include combinations of confocal or multiphoton with epifluorescence or differential interference contrast microscopes to capture light emission restricted to the focal plane as well as capturing a widefield view, either simultaneously or sequentially without having to re-orient or replace the specimen. Other options also include setting up a microscope system that combines confocal and 2P excitation imaging modes, or 2P excitation and second-harmonic generation (SHG) imaging. Although these applications tend to serve narrow and specific purposes, they may allow for imaging of local versus global Ca^{2+} signaling, or Ca^{2+} signaling in combination with e.g. metabolic parameters by using 2P excitation to excite metabolites such as NADH and FAD, or collagen that in particular contributes to the SHG signal (Masters 2006). A final example of multimodal microscopy techniques that may successfully be combined involves FRET and FLIM imaging to quantify FRET between two fluorophores, as in the case of the Ca^{2+}-sensitive cameleon described above. These examples are not exhaustive, but serve to illustrate the potential of combining different fluorophores or microscopy modalities in order to gain information of a more complex nature.

References

Bers DM. Cardiac excitation-contraction coupling. Nature 2002;90:182-189.

Bestvater F, Spiess E, Stobrawa G, Hacker M, Feurer T, Porwol T, Berchner-Pfannschmidt U, Wotzlaw C, Acker H. Two-photon fluorescence absorption and emission spectra of dyes relevant for cell imaging. J Microsc 2002;208:108-115.

Bliton C, Lechleiter J, Clapham DE. Optical modifications enabling simultaneous confocal imaging with dyes excited by ultra-violet and visible wavelength light. J Microsc 1993;169:15-26.

Bootman MD, Collins TJ, Peppiatt CM, Prothero LS, MacKenzie L, De Smet P, Travers M, Tovey SC, Seo JT, Berridge MJ, Ciccolini F, Lipp P. Calcium signalling - an overview. Semin Cell Dev Biol 2001;12:3-10.

Bullen A. Microscopic imaging techniques for drug discovery. Nat Rev Drug Discov 2008;7:54-67.

Callamaras N, Parker I. Construction of a confocal microscope for real-time x-y and x-z imaging. Cell Calcium 1999;26:271-279.

Cleemann L, Di Massa G, Morad M. Ca^{2+} sparks within 200 nm of the sarcolemma of rat ventricular cells: evidence from total internal reflection fluorescence microscopy. Adv Exp Med Biol 1997;430:435-454.

Conchello JA, Kim JJ, Hansen EW. Enhanced 3D reconstruction from confocal scanning microscope images. II: depth discrimination vs. signal-to-noise ratio in partially confocal images. Appl Opt 1994;34:3576-3588.

Conchello JA, Lichtman JW. Optical sectioning microscopy. Nat Methods 2005;2:920-931.

Cox G, Sheppard CJR. Practical limits of resolution in confocal and non-linear microscopy. Microsc Res Tech 2004;63:18-22.

Diaz ME, Trafford AW, Eisner DA. The effects of exogenous calcium buffers on the systolic calcium transient in rat ventricular myocytes. Biophys J 2001;80:1915-1925.

Denk W, Strickler J, Webb W. Two-photon laser scanning fluorescence microscopy. Science 1990;248:73-76.

Diels JC, Fontaine JJ, McMichael IC, Simoni F. Control and measurement of ultrashort pulse shapes (in amplitude and phase) with femtosecond accuracy. Appl Opt 1985;24:1270-1282.

Fast V, Idekker R. Simultaneous optical mapping of transmembrane potential and intracellular calcium in myocyte cultures. J Cardiovasc Electrophysiol 2000;11:547-556.

Hanley QS, Werweer PJ, Gemkow MJ, Arndt-Jovin D, Jovin TM. An optical sectioning programmable array microscope implemented with a digital micromirror device. J Microsc 1999;196:317-331.

Heintzmann R, Sarafis V, Munroe P, Nailon J, Hanley QS, Jovin TM. Resolution enhancement by subtraction of confocal signals taken at different pinhole sizes. Micron 2003;34:293-300.

Helmchen F, Denk W. Deep tissue two-photon microscopy. Nat Methods 2005;2:932-940.

Jares-Erijman EA, Jovin TM. FRET imaging. Nat Biotech 2003;21:1387-1395.

Kettlewell S, Cabrero P, Nicklin SA, Dow JAT, Davies S, Smith GL. Changes of intra-mitochondrial Ca^{2+} in adult ventricular cardiomyocytes examined using a novel fluorescent indicator targeted to mitochondria. J Mol Cell Cardiol 2009;46:891-901.

Kim HM, Kim BR, An MJ, Hong JHm Lee KJ, Cho BR. Two-photon fluorescent probes for long-term imaging of calcium waves in live tissue. Chemistry 2008;14:2075-2083.

Levitt JA, Matthews DR, Ameer-Beg SM, Suhling K. Fluorescence lifetime and polarization-resolved imaging in cell biology. Curr Opin Biotech 2009;20:28-36.

Lichtman JW, Conchello JA. Fluorescence microscopy. Nat Methods 2005;2:910-919.

Loughrey CM, MacEachern KE, Cooper J, Smith GL. Measurement of the dissociation constant of Fluo-3 for Ca^{2+} in isolated rabbit cardiomyocytes using Ca^{2+} wave characteristics. Cell Calcium 2003;34:1-9.

Maravall M, Mainen ZF, Sabatini BL, Svoboda K. Estimating intracellular calcium concentrations and buffering without ratioing. Biophys J 2000;78:2655-2667.

Mashanov GI, Tacon D, Knight AE, Peckham M, Molloy JE. Visualizing single molecules inside living cells using total internal reflection fluorescence microscopy. Methods 2003;29:142-152.

Masters BR. Confocal microscopy and multiphoton excitation microscopy. The genesis of live cell imaging. The international society for optical engineering press, Bellingham, WA, USA. 2006.

Miyawaki A, Llipos J, Heim R, McCaffery JM, Adams JA, Ikura M, Tsien RY. Fluorescent indicators for Ca^{2+} based on green fluorescent proteins and calmodulin. Nature 1997;388:882-887.

Miyawaki A, Mizuno H, Nagai T, Sawano A. Development of genetically encoded fluorescent indicators for calcium. Methods Enzym 2003;360:202-225.

Nagai T, Sawano A, Park ES, Miyawaki A. Circularly permuted green fluorescent proteins engineered to sense Ca^{2+}. Proc Natl Acad Sci USA 2001;98:3197-3202.

Ogden D (ed). Microelectrode techniques. The Plymouth workshop handbook, 2nd edition. The company of biologists LTD, Cambridge, UK. 1994.

Ogden D, Khodakhah K, Carter T, Thomas M, Capiod T. Analogue computation of transient changes of intracellular free Ca^{2+} concentration with the low affinity Ca^{2+} indicator furaptra during whole-cell patch-clamp recording. Pflugers Arch 1995;429:587-591.

Poenie M. Alteration of intracellular Fura-2 fluorescence by viscosity: a simple correction. Cell Calcium 1990;11:85-91.

Sanders R, Draaijer A, Gerritsen HC, Houpt PM, Levine YK. Quantitative pH imaging in cells using confocal fluorescence lifetime imaging microscopy. Anal Biochem 1995;227:302-308.

Tanaami T, Otsuki S, Tomosada N, Kosugi Y, Shimizu M, Ishida H. High-speed 1-frame/ms scanning confocal microscope with a microlens and a Nipkow disk. Appl Opt 2002;41:4704-4708.

Thomas D, Tovey S, Collins TJ, Bootman MD, Berridge MJ, Lipp P. A comparison of fluorescent Ca^{2+} indicator properties and their use in measuring elementary and global Ca^{2+} signals. Cell Calcium 2000;28:213-223.

Tsien RY. New calcium indicators and buffers with high selectivity against magnesium and protons: design, synthesis, and properties of prototype structures. Biochemistry 1980;19:2396-2404.

Tsien RY, Bacskai BJ. Video-rate confocal microscopy. In Pawley JB (ed), Handbook of biological confocal microscopy. Plenum press, New York, USA. 1995.

Wang E, Babbey CM, Dunn KW. Performance comparison between the high-speed Yokogawa spinning disc confocal system and single-point scanning confocal systems. J Microsc 2005;218:148-159.

Webb R. Theoretical basis of confocal microscopy. Methods Enzymol 1999:307:3-20.

Willig KI, Rizzoli SO, Westphal V, Jahn R, Hell SW. STED microscopy reveals that synaptotagmin remains clustered after synaptic vesicle exocytosis. Nature 2006;440:935-939.

Wilson T, Juskaitis R, Neil MA, Kozubek M. Confocal microscopy by aperture correlation. Opt Lett 1996 ;21 :1879-1881.

Wokosin DL, Loughrey CM, Smith GL. Characterization of a range of Fura dyes with two-photon excitation. Biophys J 2004;86:1726-1738.

Xu C, Zipfel WR, Shear JB, Williams RM, Webb WW. Multiphoton fluorescence excitation: new spectral windows for biological nonlinear microscopy. Proc Natl Acad Sci USA 1996;93:10763-10768.

Zipfel WR, Williams RM, Webb WW. Nonlinear magic: multiphoton microscopy in the biosciences. Nat Biotechnol 2003;21:1369-1377.

Figure 1

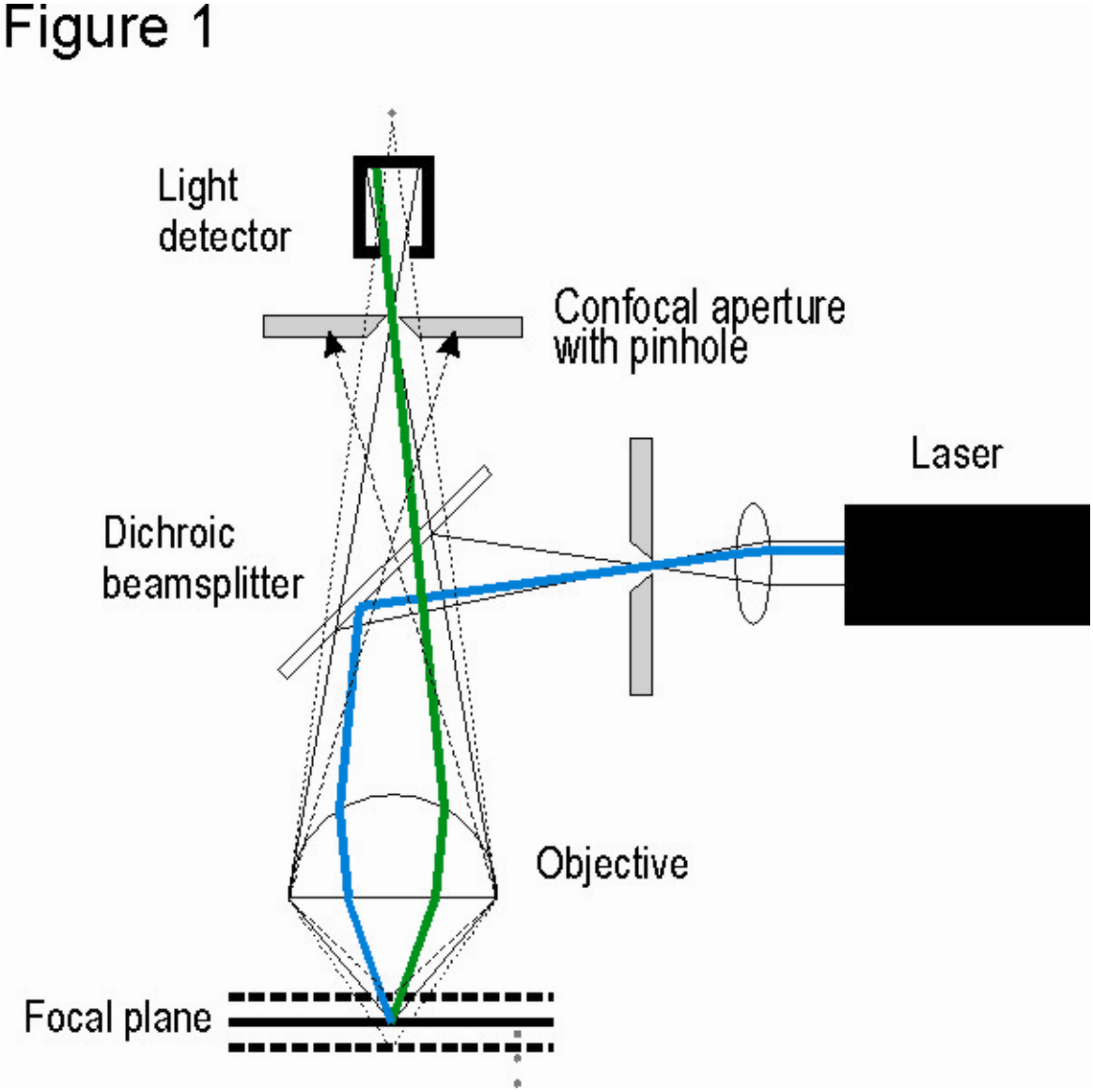

Figure 1: Overview of the optical pathway of a confocal microscope. The blue path illustrates the excitation light, whereas the green path illustrates the emitted fluorescence light. Note that the confocal aperture with the pinhole in front of the light detector (usually a photomultiplier tube (PMT)) blocks out-of-focus light.

Figure 2

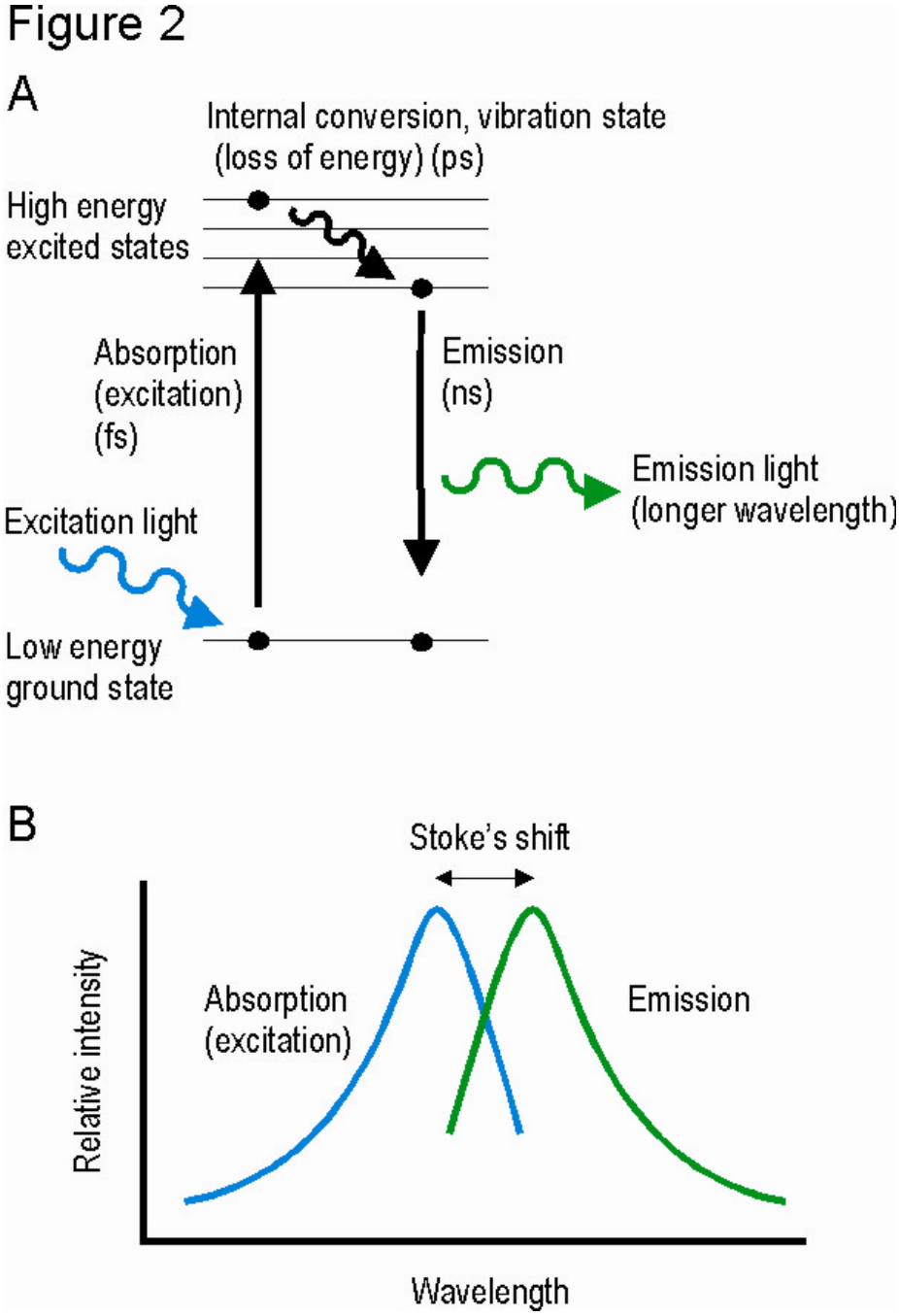

Figure 2: A: A Jablonski diagram showing the energy states of a given fluorophore, including the process of absorption and emission of longer wavelength light upon excitation. The duration of each state is also indicated. B: The absorption and emission spectra of a given fluorophore including the Stoke's shift due to emission of a longer wavelength photon upon excitation of the fluorophore.

Figure 3

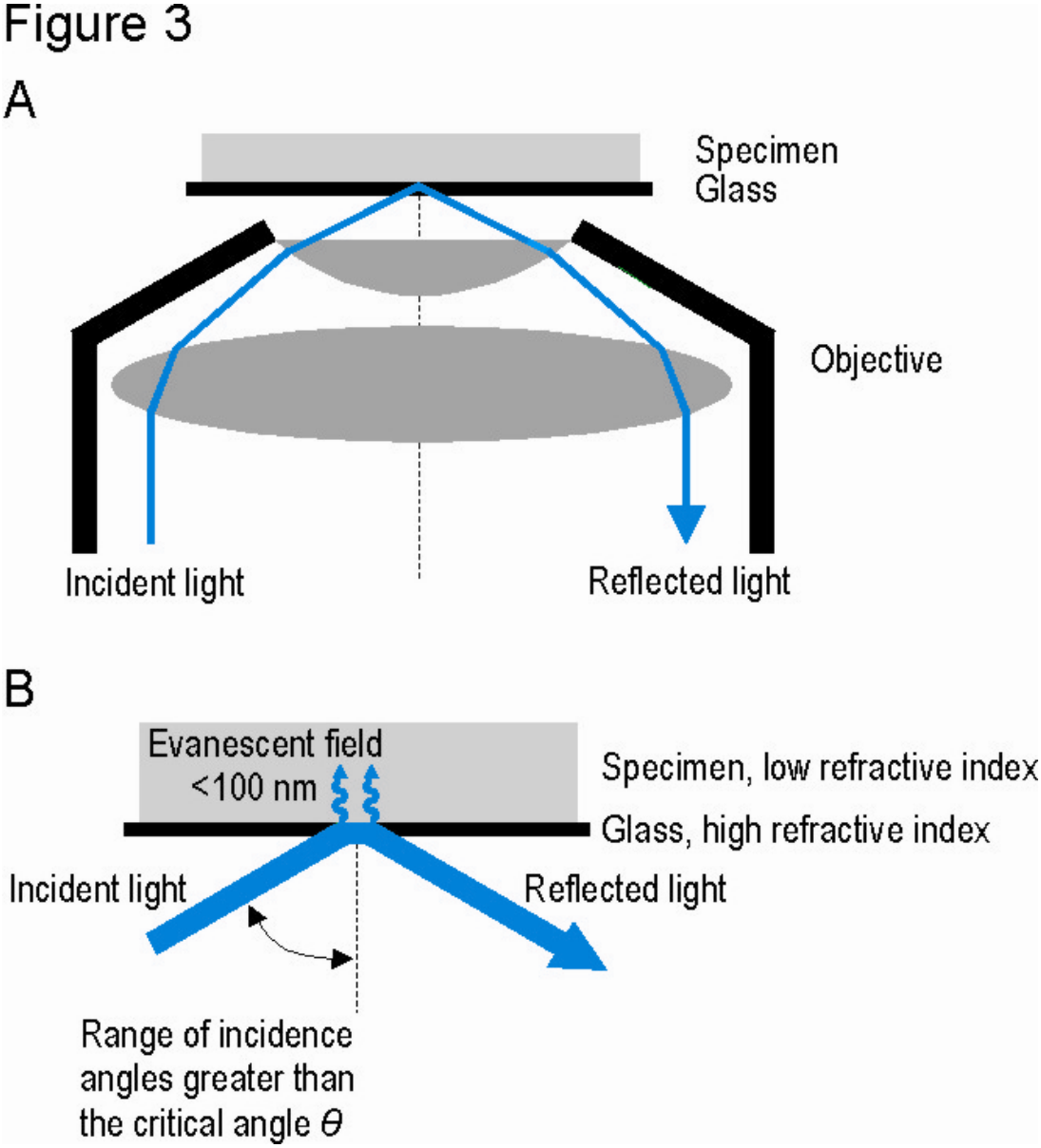

Figure 3: Total internal reflection fluorescence (TIRF) microscopy. A: Overview including the incident and reflected laser light paths within the objective. B: Once the incident light reaches a medium with a lower refractive index at an angle greater than the critical angle θ, the incident light does not penetrate the specimen, but an electromagnetic field is created that penetrates up to ~100 nm above the surface, called an evanescent wave. This may excite fluorophores within the range of the evanescent wave.

Figure 4

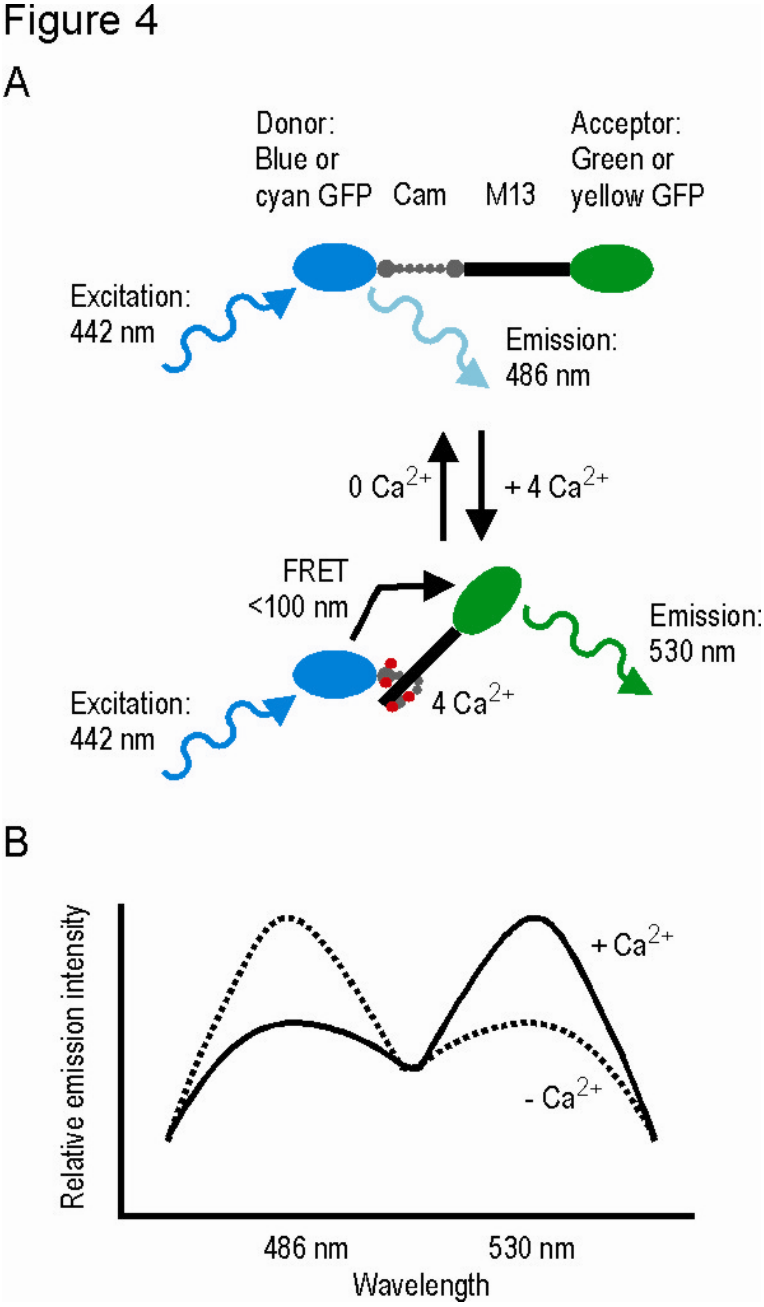

Figure 4: Cameleon-based förster resonance energy transfer (FRET). A: Schematic of the cameleon in the absence and presence of Ca^{2+}; note the conformational change in the calmodulin (Cam) and the Cam-binding domain of myosin light chain kinase (M13) upon binding to Ca^{2+} that allows for FRET between the donor and acceptor green fluorescent protein (GFP) mutants. B: The relative emission intensities at different wavelengths indicate whether or not Ca^{2+} is present, and hence FRET occurs.

Figure 5

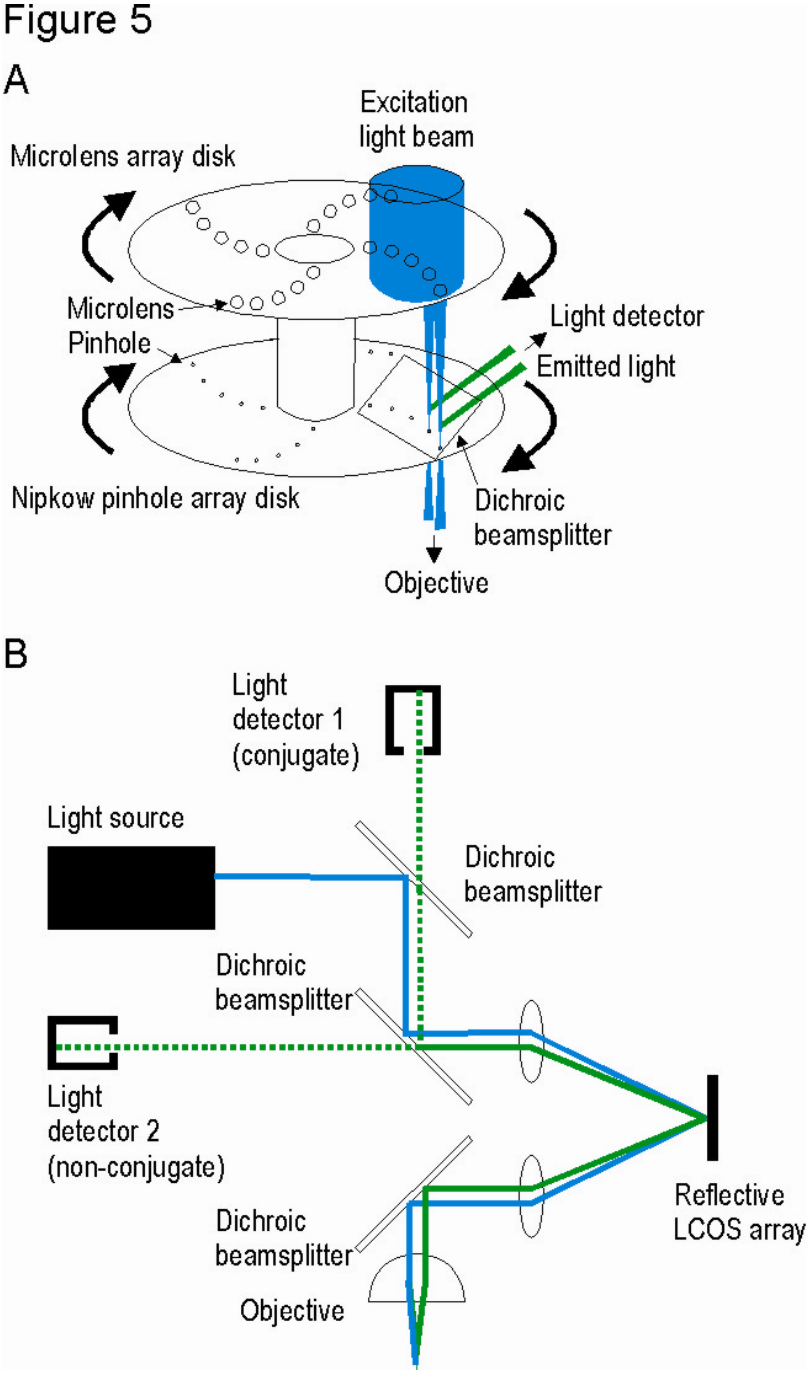

Figure 5: A: Nipkow spinning disk. The figure highlights two lightbeams reaching the specimen and the light detector, but in reality multiple beams reach the specimen and the light detector simultaneously. B: The optical pathway of a programmable matrix microscope. The liquid crystal on silicon (LCOS) array consists of numerous µm-sized liquid crystal "pixels" that can be switched independently to reflect the lightbeam onto multiple spots simultaneously.

Figure 6

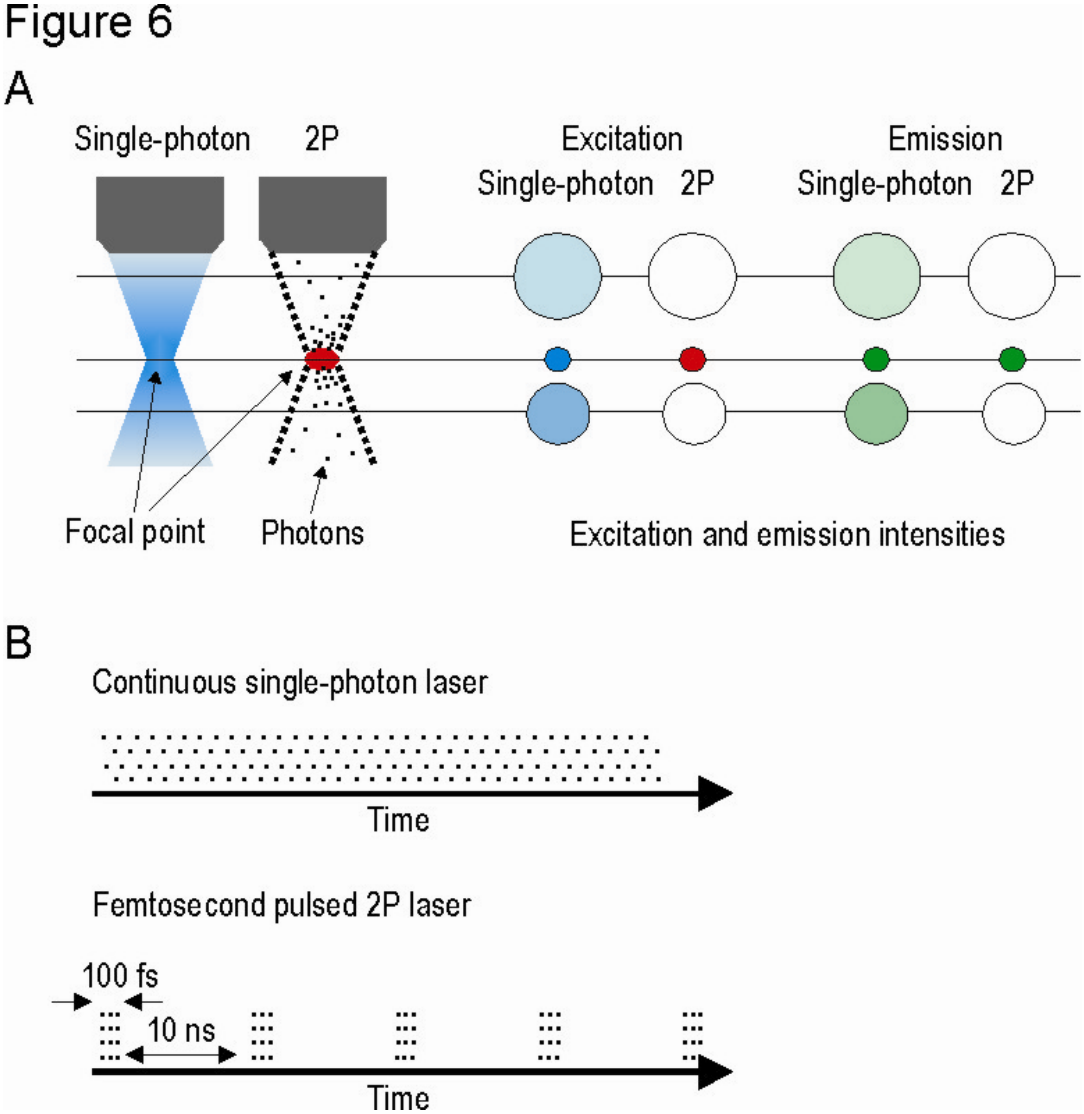

Figure 6: Two-photon (2P) excitation microscopy, including a comparison to single-photon confocal microscopy. A: Schematic of illumination lightbeams, in which excitation occurs along the whole z-axis with single-photon confocal microscopy; though with highest intensity at the focal point, whereas excitation is confined to a narrow area around the focal point with 2P microscopy. Correspondingly, emission occurs along the entire z-axis with confocal microscopy; though out-of-focus light is blocked by the confocal aperture, whereas emission is confined to a narrow area around the focal point with 2P excitation microscopy. B: Schematic of the continuous laser used for single-photon excitation and a pulsed titanium:sapphire (Ti:Sapphire) laser used for 2P excitation.

Figure 7

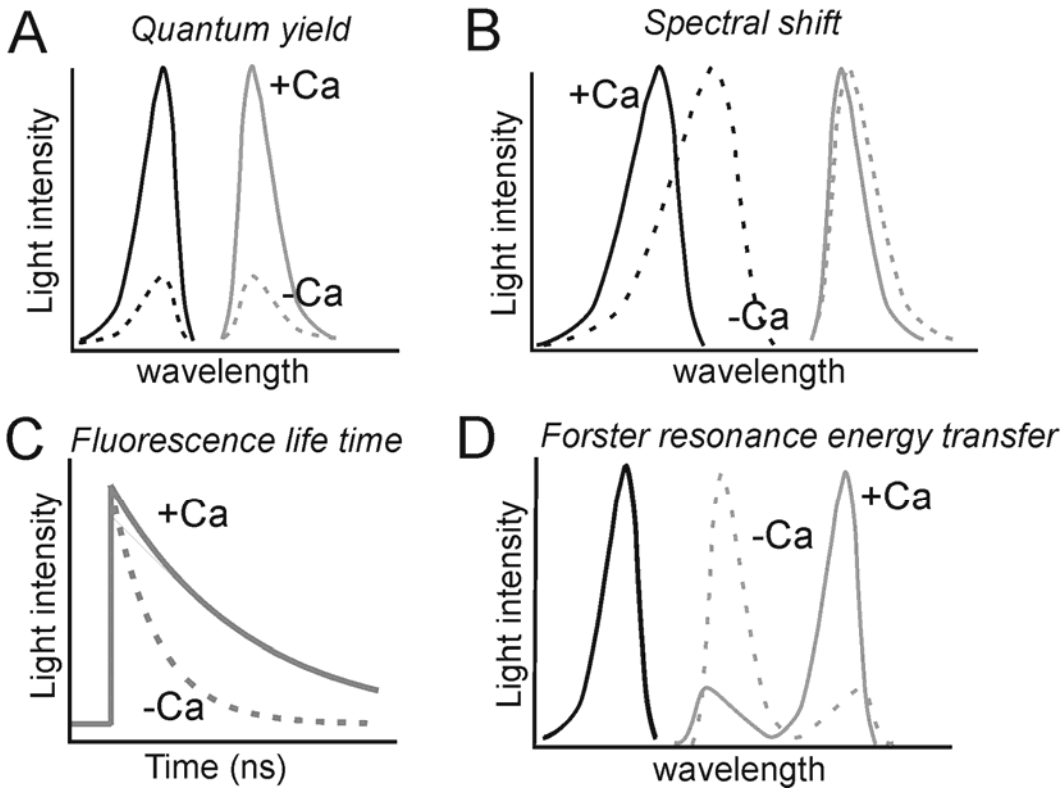

Figure 7: Major categories of fluorescence properties of Ca^{2+} indicators. A: Change in dye absorbance and quantum yield generates a Ca^{2+} sensitive change in the fluorescence intensity (examples Fluo-3/4 Rhod-2, Oregon Green and Fura-Red (inverse relationship). B: Spectral shift in the excitation spectrum as a result of Ca^{2+} binding to an indicator allows ratiometric measurements (example Fura-2/3/4/6/FF). C: Changes in fluorescence life time as a result of Ca^{2+} binding to an indicator; the fluorescence decays exponentially within ns of the end of excitation. The rate of decay is Ca^{2+} dependant; for example the decay of Ca^{2+}-bound Fluo-3 fluorescence is faster than the decay of unbound Fluo-3. D: Change in förster resonance energy transfer (FRET) efficiency as a result of Ca^{2+} binding to either the acceptor or donor proteins; Ca^{2+} binding changes the distance between the two linked fluorescent proteins. The distance between the donor and acceptor proteins determines the degree of FRET, an increase in FRET efficiency causes a decrease in donor fluorescence and an increase in acceptor fluorescence. Black lines indicate excitation spectra and grey lines indicate emission spectra. Dotted lines represent the Ca^{2+}-free form of the dye, whereas solid lines represent the Ca^{2+}-bound form of the dye.

Figure 8

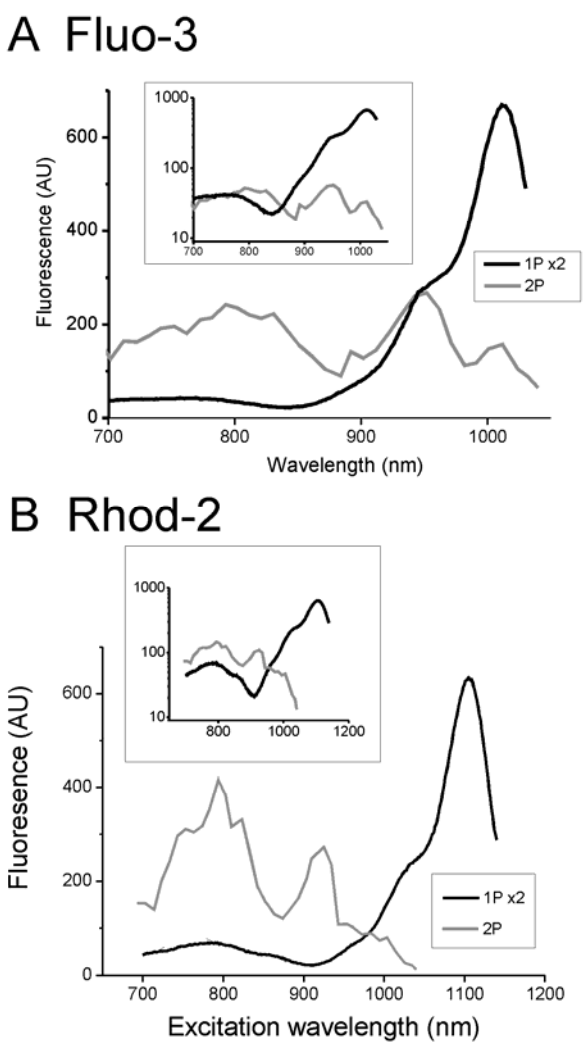

Figure 8: Excitation spectra of Ca^{2+} bound forms of A: Fluo-3 and B: Rhod-2 spectra. Emitted fluorescence was collected at 500-650 nm (Fluo-3) and 550-650 nm (Rhod-2). Black line represents the single-photon (1P) excitation spectra measured on a Perkin-Elmer spectrophotometer (2 nm slit width); the 1P wavelength has been scaled by a factor of 2 (x2) to generate comparable wavelengths to two-photon (2P) spectra. Grey line represents the 2P excitation spectrum of an equivalent concentration of dye (10 μM); excitation light was provided by a Coherent Chameleon XP Ti-Sapphire laser attached to a Zeiss 510 upright laser scanning microscope. Laser power was altered at each wavelength to ensure equivalent excitation power across the excitation wavelengths.

Figure 9

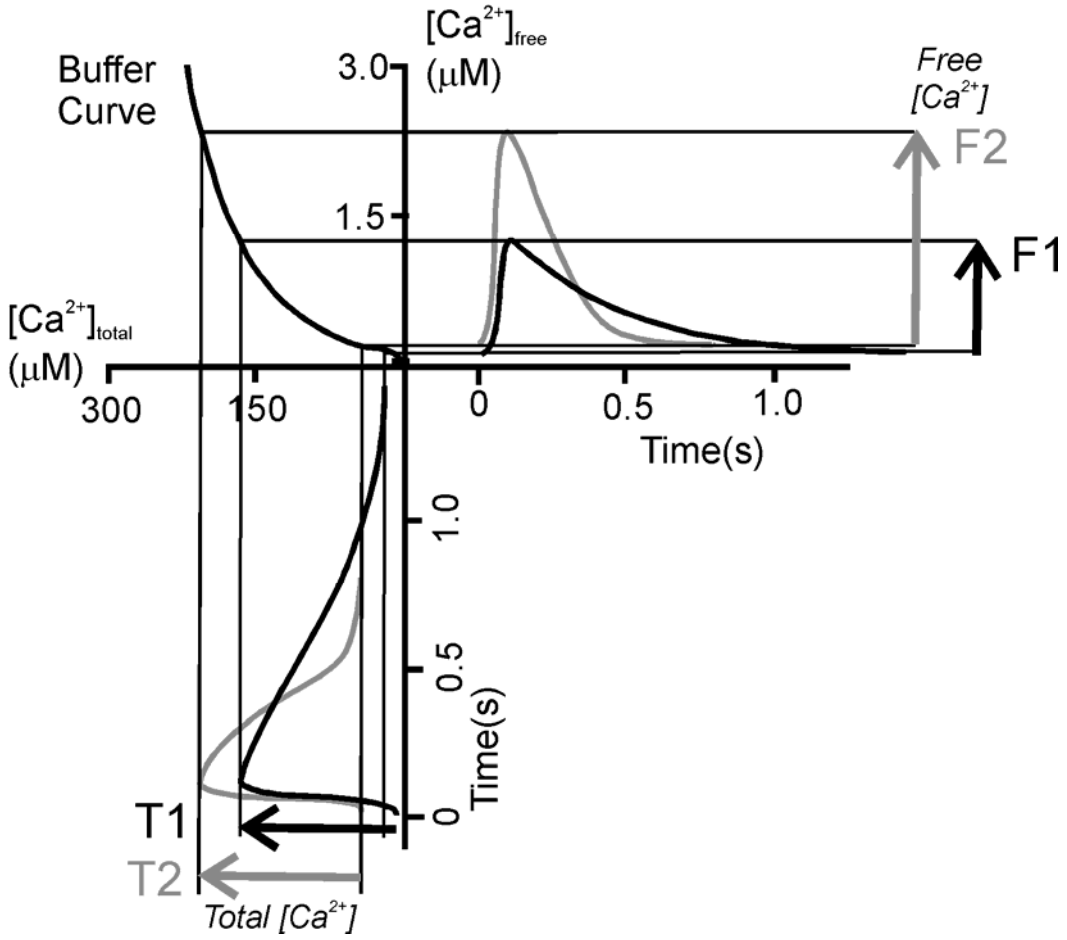

Figure 9: Illustration of the conversion of increments in total cellular Ca^{2+} to free Ca^{2+} signal using the cellular buffer power. Increase of the total cellular Ca^{2+} by equivalent amounts (T1 & T2) causes a rise of free [Ca^{2+}] of F1 and F2 due to differences in the background [Ca^{2+}]. Cellular Ca^{2+} buffer is illustrated by the relationship between total cellular Ca^{2+} and free Ca^{2+}. Note that while the amplitude of the transient increase in free [Ca^{2+}] depends on the increase in total Ca^{2+} and the cellular buffer power, the time course of the decrease will depend on the extent of activation of cellular Ca^{2+} pumps and exchangers. Generally the rate of these processes depends on the free [Ca^{2+}], therefore the decay of the Ca^{2+} transients of different amplitudes may differ substantially.

Figure 10

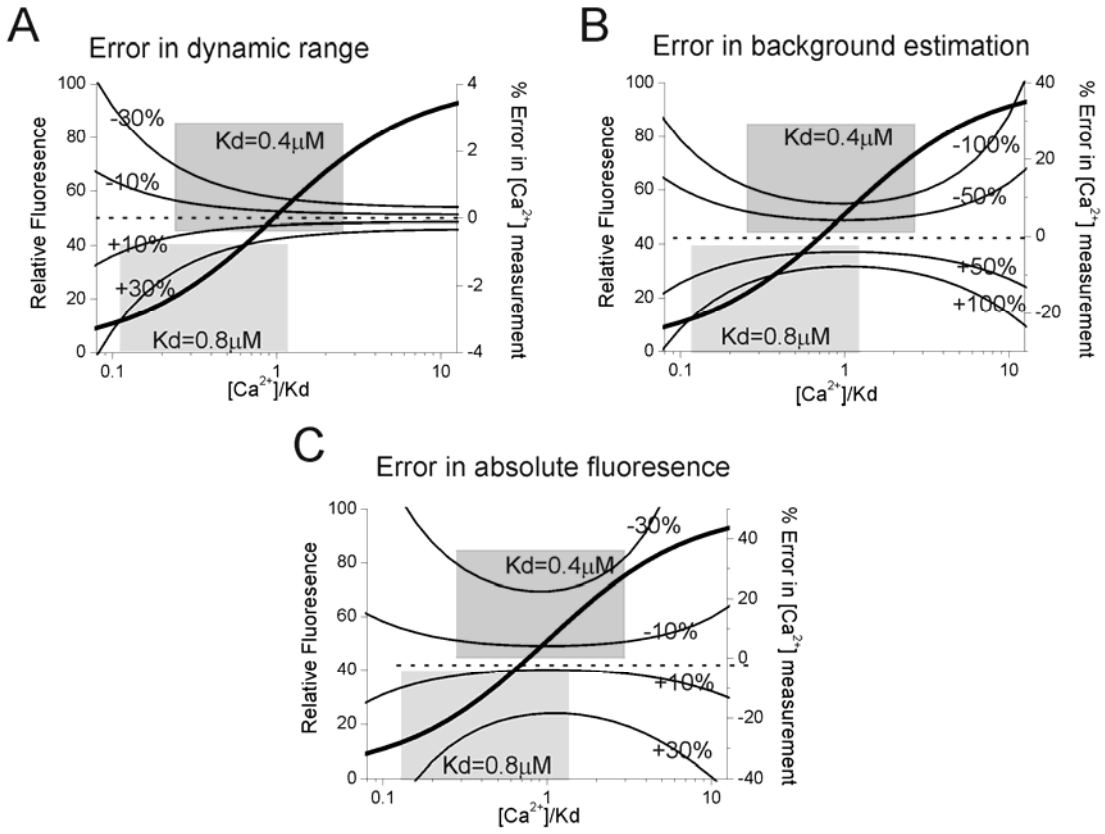

Figure 10: $[Ca^{2+}]$ calibration errors. A: Error due to changes in background fluorescence plotted against varying $[Ca^{2+}]$ values normalized by the indicator K_d (0.4 μM, Fluo-3 and 0.8 μM, Fluo5F). Dynamic range of the dye was set at 100 (maximum attributable to Fluo-3). A typical cellular Ca^{2+} concentration range is highlighted by grey boxes (100 nM to 1 μM) for each of the two K_d values. The left axis (thick line) highlights the relative fluorescence versus $[Ca^{2+}]$. The right axis (thin lines) represents the % error in $[Ca^{2+}]$ due to variations in the intracellular background. Two levels of background fluorescence were considered: (i) background fluorescence is equal in magnitude to F_{min}; errors of +/- 50% and +/- 100% background were considered, and (ii) background fluorescence is equal to 5x F_{min}; errors of +/- 10% and +/- 20% of background fluorescence. These two combinations of background and errors superimpose exactly (i.e. +/-50% superimposes on +/-10% and +/-100% superimposes on +/- 20%) to produce the 4 error lines shown. B: Error in absolute fluorescence levels; errors of +/- 10% and +/- 30% are shown. C: Error in dynamic range of Fluo- and Rhod-based dyes; errors of +/- 10% and +/- 30% are shown.

Figure 11

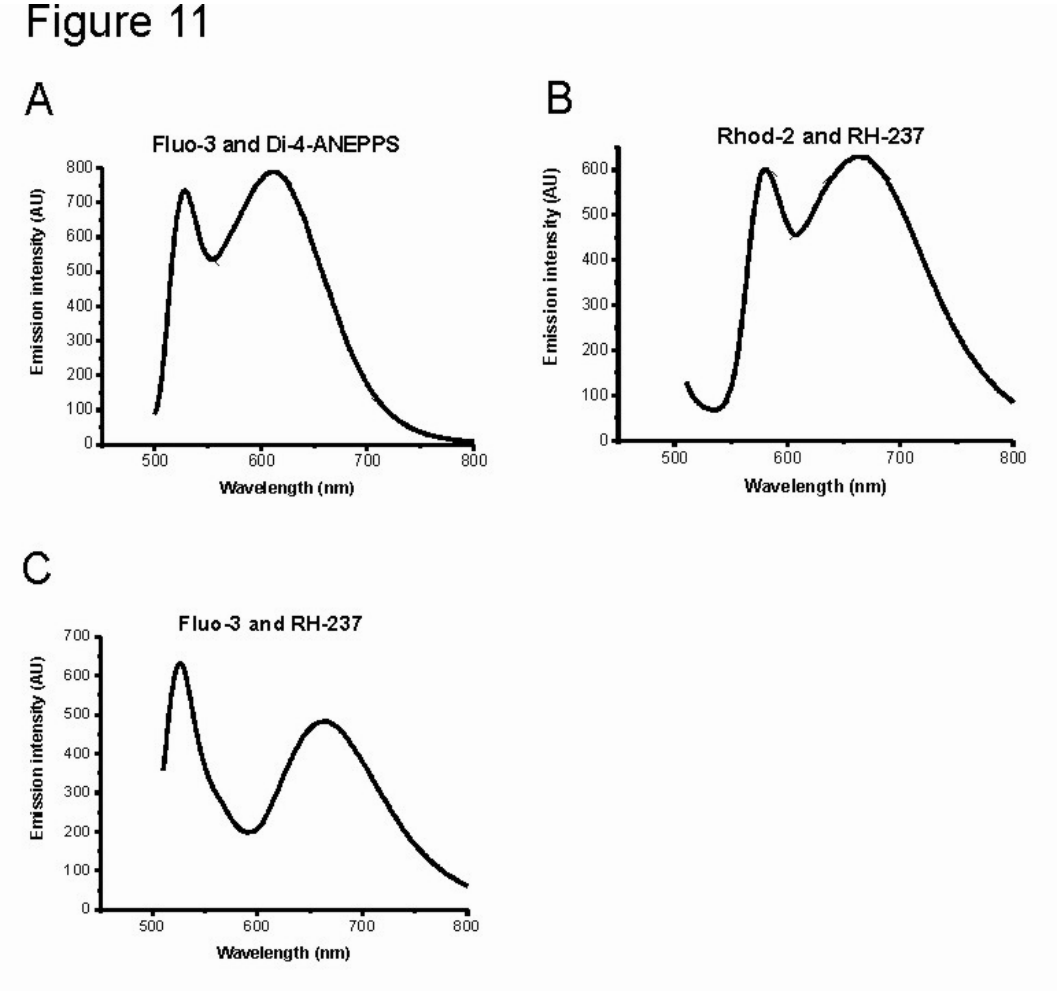

Figure 11: Single-photon emission spectra of voltage sensitive Di-4-ANEPPS and RH-237, and Ca^{2+}-sensitive Fluo-3 and Rhod-2 dyes. The following emission spectra were obtained by spectrophotometry after simultaneously loading cardiac muscle cells in a high Ca^{2+} solution (60 μM) with Ca^{2+}- and voltage-sensitive dyes and exciting at 488 nm. The presence of intact excitable cells in a Ca^{2+}-rich environment provides substrate for both Ca^{2+}- and voltage-sensitive dyes. A: Fluo-3 (Ca^{2+}; first peak) and Di-4-ANEPPS (voltage; second peak). B: Rhod-2 (Ca^{2+}; first peak) and RH-237 (voltage; second peak). C: Fluo-3 (Ca^{2+}; first peak) and RH-237 (voltage; second peak).